Mechanistic Comparison of High-Fidelity and Error-Prone DNA Polymerases and Ligases Involved in DNA Repair

Alexander K. Showalter, Brandon J. Lamarche, Marina Bakhtina, Mei-I Su, Kuo-Hsiang Tang, and Ming-Daw Tsai*

Departments of Chemistry and Biochemistry, The Ohio State University, Columbus, Ohio, and Genomics Research Center, Academia Sinica, Taiwan

Received May 13, 2005

Contents

1. Introduction

1.1. Scope of This Review

Discovered in the early 1970s, DNA polymerase β (Pol β) was the first mammalian DNA repair polymerase to be characterized. Its relatively small size (39 kD) and the fact that it lacks an exonuclease proofreading activity make it a tractable system for studying the mechanism by which fidelity is achieved during DNA polymerization. Though extensive studies in ours and other laboratories (see the review by Wilson[1] in this issue) have revealed this enzyme to display moderately high fidelity, a consensus has not yet been reached regarding the mechanism by which this is accomplished. Drawing on both structural data and kinetic analyses, herein we present an overview of the Pol β reaction mechanism and discuss its implications for the fidelity of nucleotide incorporation. Note that the fidelity of DNA polymerases in general was recently reviewed by Kunkel[2] and Joyce and Benkovic,[3] and its structural origin was also the subject of another review by Beard and Wilson.[4] Subsequently, without duplicating other reviews on the subject,[5−7] we consider structural and functional data for some of the recently discovered error-prone DNA polymerases including the African swine fever virus (ASFV) DNA polymerase X (Pol X), and by comparison with higher fidelity enzymes such as Pol β, we draw some conclusions about the mechanistic features contributing to relaxed polymerization fidelity. In the latter part of this review we then discuss fidelity as it pertains to DNA ligation. Participation of an error-prone polymerase in DNA repair processes can generate DNA nicks possessing 3′-OH mismatches. The extent to which these mismatches are discriminated against by DNA ligases, and the mechanisms of discrimination are discussed by comparison of a broad range of enzymes including those from human, ASFV, and bacteriophage T4. Finally, the complete ASFV-encoded DNA repair system, which displays low fidelity at both the DNA repair polymerization and nick ligation steps, is presented and the biological implications discussed.

1.2. Types of Mechanism: Chemical, Kinetic, and Structural

Depending on the context in which it is employed, the term "mechanism" frequently has different connotations; this

10.1021/cr040487k CCC: $59.00
Published on Web 01/25/2006

Alexander K. Showalter received a B.S. degree in biochemistry from the State University of New York in 1996 and a Ph.D. in chemistry from The Ohio State University in 2002. Working under the supervision of Ming-Daw Tsai, his doctoral research focused on DNA polymerase enzymology. He currently works in the pharmaceutical industry.

Brandon J. Lamarche earned a B.S. in chemistry from Westmont College in 1999. Working in the laboratory of Ming-Daw Tsai, he received a Ph.D. in chemistry from The Ohio State University in 2005. His research interests involve the enzymology of DNA repair.

Marina Bakhtina received a B.S. in molecular biology from Novosibirsk State University (Russia) in 1993. She worked as a research associate for four years in the Institute of Molecular Biology (SRC VB "Vector") and subsequently earned an M.S. in philosophy from Novosibirsk State University in 1999. She is currently a graduate student in Ming-Daw Tsai's group at The Ohio State University, where her doctoral research is focused on the kinetic mechanism of DNA polymerase fidelity.

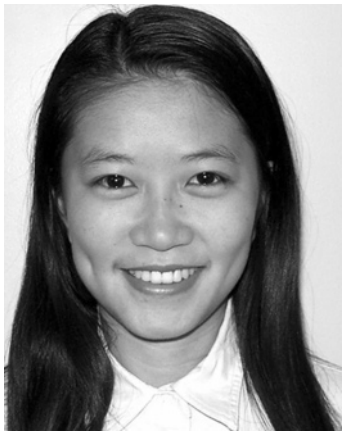

Mei-I Su received her B.S. degree from the National Taiwan University in 1997 and a Ph.D. in chemistry from The Ohio State University in 2004, under the supervision of Dr. Ming-Daw Tsai. She is currently a postdoctoral researcher in the Tsai group (working at both The Ohio State University and the Genomics Research Center of Academia Sinica, Taiwan), where she focuses on structural studies of DNA polymerase X.

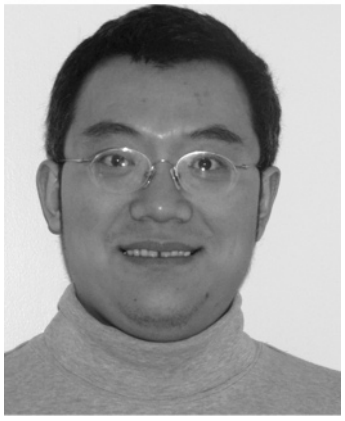

Kuo-Hsiang Tang received a B.S. from Tamkang University in 1990, an M.S. working with Dr. Yeun-Min Tsai at the National Taiwan University in 1992, and a Ph.D. (major in biochemistry and minor in pharmaceutical science) from the University of Wisconsin, Madison, in 2002, working with Dr. Perry A. Frey. After postdoctoral studies under the supervision of Dr. Daniel Herschlag at Stanford University, in September 2004 he joined Tsai's group (working at both The Ohio State University and the Genomics Research Center of Academia Sinica, Taiwan), where his research focuses on the development and application of various biophysical approaches for structural analyses of DNA polymerases.

is particularly true at the interface between chemical and biological research. Thus, it may be useful to define precisely what the term will mean within the scope of this review. We split the term mechanism into three specific varieties: chemical mechanism, kinetic mechanism, and structural mechanism. It is important, however, to keep in mind that these are intimately related to one another. Since different labs investigate the three types of mechanism using different techniques, the correlation between them is frequently neglected, and this can result in different interpretations of the mechanism of catalysis for a given enzyme.

The chemical mechanism refers specifically to the covalent transformation or series of covalent transformations which directly achieve the overall reaction. It can also refer to related concepts, such as the stereochemistry of the reaction (e.g. whether it proceeds with inversion or retention) or the nucleophilicity or electrophilicity of the reaction (or in the terminology of phosphoryl transfer, its associative or dissociative nature). Largely on the basis of crystal structures, most features of the chemical mechanism of DNA polymerization have been elucidated or confidently surmised. The reaction consists of a single nucleotidyl transfer utilizing two magnesium ions that are coordinated, in part, by three

Ming-Daw Tsai received a B.S. degree in chemistry from the National Taiwan University in 1972, received a Ph.D. in medicinal chemistry from Purdue University in 1978, and joined the faculty of The Ohio State University in 1981. He is currently the Kimberly Professor of Chemistry and Professor of Biochemistry. He established the Chemistry–Biology Interface Training Program of OSU in 1996 and served as its director through 2003. Since 1995 he has also directed OSU's Office of Research Campus Chemical Instrument Center. In 2003 Tsai became a Distinguished Research Fellow in the Genomics Research Center of Academia Sinica, Taiwan, where he leads a research team in functional genomics and oversees the National Core Facilities Program in Genomic Medicine. Tsai has published nearly 200 articles in chemical and biological journals. His honors include an Alfred P. Sloan Fellowship (1983–1985), the Camille and Henry Dreyfus Teacher–Scholar Award (1985–1990), the Distinguished Scholar Award of The Ohio State University (1992), and an Elected Fellow of the American Association for the Advancement of Science (1992). His current research interests are in the structure and mechanism of proteins and enzymes involved in DNA damage repair and cancer.

conserved active site aspartate residues. While one magnesium ion is recruited to the active site via its chelation by the triphosphate moiety of the incoming dNTP, the other magnesium ion (often called the catalytic magnesium ion) is coordinated by both the 3′-OH nucleophile of the primer and the α-phosphate of the incoming dNTP (Figure 1); collectively, these two ions serve to stabilize what is presumably an electron-rich, associative transition state. Since the chemical mechanism is not expected to differ significantly for low-fidelity enzymes vs the more thoroughly studied high-fidelity enzymes, it will not be a focus of this review—although it will be mentioned, where appropriate.

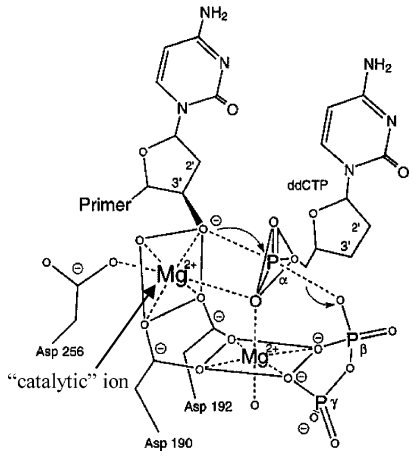

Figure 1. Schematic diagram of the Pol β active site showing the two magnesium ions required for catalysis. By structural and kinetic studies, the different roles of both ions have been dissected. The first ion, frequently called the *nucleotide-binding ion*, is considered to be associated with the incoming dNTP in the kinetic scheme. The second ion, often called the *catalytic ion*, binds the active site independently of the incoming nucleotide. Adapted with permission from ref 14. Copyright 1997 American Chemical Society.

The kinetic mechanism refers to the rates of all the steps (binding/dissociation, conformational, and chemical) in the reaction pathway or, viewed alternatively, to the change in free energy associated with each step. For deciphering kinetic mechanisms, pre-steady-state analyses are superior to steady-state analyses in that the former can provide rate information for the interconversion of reaction intermediates. Accordingly, when discussing kinetic mechanisms, this review will focus mainly on pre-steady-state kinetic results.

The structural mechanism refers to all structures in the reaction pathway and their interconversion, with particular emphasis on noncovalent interactions between enzyme and substrates/products/cofactors and any global changes in enzyme conformation caused by those interactions. This review considers advances in understanding of structural mechanism that have been made within the past five years, with a focus on those structures most relevant to kinetic and chemical mechanisms.

1.3. Mechanism of Fidelity

Prior to discussing the "mechanism of fidelity" as it relates to DNA polymerization, it is first necessary to define fidelity. DNA polymerase fidelity has been measured in different ways, including (a) comparison of kinetic constants for Watson−Crick and mismatched nucleotide incorporation reactions and (b) measurement of misincorporation frequency when competing nucleotides are simultaneously present.[8−10] Note that it has been pointed out that the fidelity as measured by pre-steady-state kinetic analyses is equivalent to the fidelity as measured by direct competition assays under processive conditions. Herein our focus is on pre-steady-state kinetic constants, although the analogous steady-state constants are also used, as applied to the following terms: *Catalytic efficiency* is the pseudo-second-order rate constant for product formation with a given substrate, defined as $k_{pol}/K_{d,app}$. *Fidelity* is the catalytic efficiency ratio indicative of an enzyme's propensity to select the correct nucleotide over any given incorrect nucleotide, defined as $[(k_{pol}/K_{d,app})_{cor} + (k_{pol}/K_{d,app})_{inc}]/(k_{pol}/K_{d,app})_{inc}$, where the subscripts "cor" and "inc" indicate the correct and incorrect nucleotide incorporation, respectively. Note that many researchers use a slightly different, "direct ratio" definition of fidelity: $(k_{pol}/K_{d,app})_{cor}/(k_{pol}/K_{d,app})_{inc}$. The latter definition will obviously yield a fidelity value that is one whole number lower than the fidelity value derived from the former definition, a difference which becomes significant only at very low fidelities. Short of adopting a common definition—and we believe there are arguments to be made for each candidate—it is important to note the use of both and to understand the difference it creates in numerically describing low fidelities.

The mechanism of fidelity can thus be described as "the manner in which high $(k_{pol}/K_{d,app})_{cor}$ values and low $(k_{pol}/K_{d,app})_{inc}$ values are achieved by high-fidelity polymerases" or "the manner in which comparable $(k_{pol}/K_{d,app})_{cor}$ and $(k_{pol}/K_{d,app})_{inc}$ values are achieved by error-prone polymerases". The critical question is: "how, and at which step, does the enzyme control the $(k_{pol}/K_{d,app})$ value, for both correct and incorrect dNTP incorporations?" We address this question by comparing high-fidelity and error-prone polymerases in sections 2−4. The mechanism of fidelity, as it pertains to DNA ligation, is then examined in section 5.

2. Kinetic Mechanism of DNA Polymerase β

2.1. Background

Early kinetic studies [1980s to 1990s, focused primarily on the 3′ → 5′ exonuclease-deficient Klenow fragment (exo⁻ KF)] concluded that DNA polymerases achieve dNTP selectivity (i.e. fidelity) by an induced-fit mechanism involving a rate-limiting conformational change.[8,11,12] When structural studies (late 1990s) showed a subdomain closing conformational change upon dNTP binding to the E·DNA binary complex,[13,14] it was assumed that this was the same rate-limiting conformational change previously suggested by kinetic analyses. This led to the dogma that the "open-to-closed" protein structural transition is the rate-limiting step prior to chemistry and therefore the major determinant of fidelity.[13,14] Though we initially interpreted our kinetic data for Pol β to be consistent with this mechanism,[15−17] we were forced to reevaluate this interpretation around 2000 when our kinetic and structural results collectively indicated that the subdomain closing conformational change of Pol β is *faster* than chemistry.[18] In a commentary paper in 2002 we reevaluated the theoretical and experimental bases for the induced-fit mechanism of polymerase fidelity and suggested an alternative model in which the chemical step is rate-limiting and the energetic difference between correct and mismatched dNTP incorporation at the transition state of Pol β's catalysis is the sole arbiter of its fidelity.[19] In response to this proposition, some researchers suggested that if subdomain closing is indeed a fast step, there should be another rate-limiting conformational change which is likely to be silent spectroscopically. Schlick and Wilson suggested that this slow, prechemistry step is reorientation of Arg258,[20] while Joyce and Benkovic suggested a number of possibilities.[3] In this section we consider evidence pertaining to the above models. Our focus will be on identification of the rate-limiting step through the use of substrate analogues and manipulated reaction conditions.

2.2. Stopped-Flow Fluorescence Analyses of Pol β

Pol β has been studied extensively by stopped-flow kinetic analyses. Immediately after rapid mixing of E·DNA (where DNA is a template/primer substrate) and dNTP+Mg^{2+}, the reaction's progress is monitored using either of two fluorescent probes: the enzyme's sole Trp residue at position 325 (Figure 2A) or 2-aminopurine (2AP) on the templating DNA strand (Figure 2B). Regardless of which of these probes is used, two fluorescence transitions are detected: one with a rate identical to that of dNTP incorporation, as determined by rapid-quench experiments under single-turnover conditions, and one with a rate significantly greater.[21]

The critical question, then, is: "what are the structural bases of the two fluorescence transitions?" According to the hypothesis that the subdomain closing step is rate-limiting,[8,13,14] the slow fluorescence transition should reflect the rate constant for this global conformational change. However, as described in the section that follows, the results of numerous studies indicate that the subdomain closing conformational change is associated with the fast fluorescence transition, while the rate of the slow fluorescence transition reflects the rate of the chemical step.

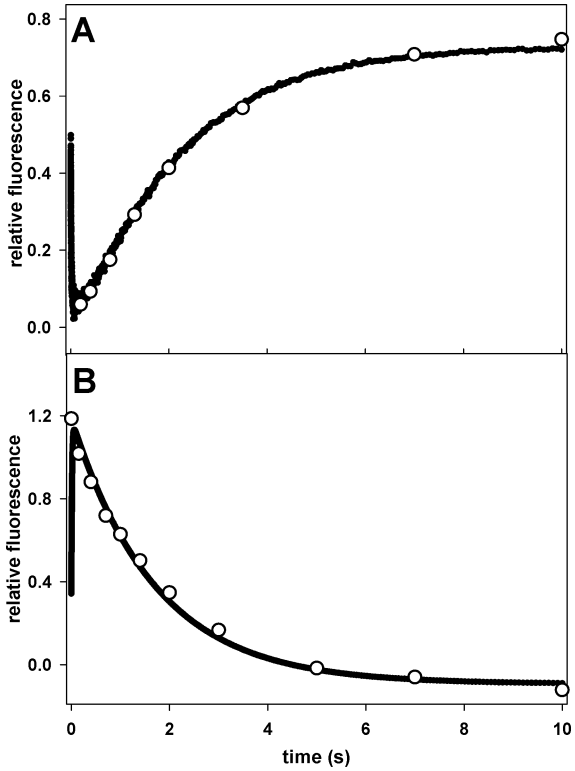

Figure 2. (A) Superimposition of rapid chemical quench (○) and tryptophan fluorescence stopped-flow (●) time courses for incorporation of dCTP (opposite to templating guanine) into a 36mer/18mer template/primer DNA substrate. The rapid quench data points fit to a single exponential with a rate constant of 0.430 s^{-1}. The stopped-flow data points fit to a double exponential with $k_1 = 64.4$ s^{-1} and $k_2 = 0.457$ s^{-1}.[21] (B) Similar assays for incorporation of dCTP (opposite to templating guanine) into a 2AP-containing 35mer/18mer template/primer DNA substrate. 2AP was located at the 20th position (from the 3′-end) of the templating 35mer, placing it one nucleotide downstream of the nascent base pair. The fluorescence change of 2AP, instead of tryptophan, was monitored; notice that the direction of the fluorescence change for 2AP is opposite to that of tryptophan. The results of the assays described in parts A and B have been reproduced under a variety of conditions and with the 2AP fluorophore located at different positions within the templating strand of the DNA substrate.[21] Part A is reproduced with permission from ref 23. Copyright 2005 American Chemical Society.

2.3. Application of Chemical Probes To Elucidate the Kinetic Mechanism

By application of numerous chemical probes, we have rigorously characterized the nature of the two phases in the Pol β stopped-flow fluorescence signal, leading us to propose the revised kinetic scheme and associated free energy diagram shown in parts A and B of Figure 3. In this scheme the fast fluorescence transition represents the E to E′ step (the dNTP-induced subdomain closure—step 2 in Figure 3), while the slow fluorescence transition reflects a conformational change, most likely subdomain reopening (step 6 in Figure 3), which is rapid relative to chemistry and thereby limited in rate by the chemical step. Evidence for this model includes the following:

(a) Alteration of reaction buffer viscosity is expected to selectively perturb macromolecular conformational (rather than chemical) steps.[22] At pH 7.0, increasing buffer viscosity selectively decreases the rate of the fast fluorescence transition, suggesting that this phase reflects a conformational

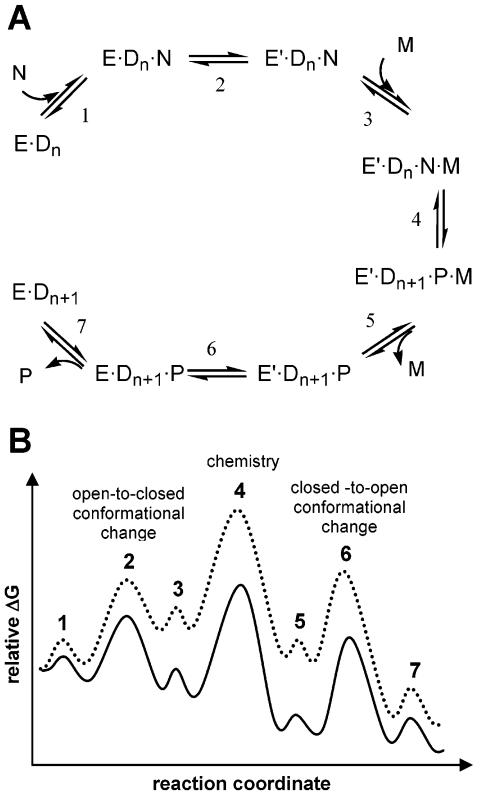

Figure 3. (A) Kinetic scheme for Polβ-catalyzed single-nucleotide incorporation. E = Pol β in the open finger conformation; E′ = Pol β in the closed finger conformation; D_n = DNA; N = M·dNTP; M = catalytic metal ion; P = M·PP_i. In the text, the *binary* complex refers to the E·D_n state, while the *ternary* complex refers to either the E′·D_n·N state or the E′·D_n·N·M state.[18,21] (B) Possible free energy profiles for correct (—) and mismatched (···) nucleotide incorporation by Pol β. The number associated with each peak denotes the corresponding microscopic step in the kinetic scheme of part A.

change associated with progression from the binary to the ternary complex.[23]

(b) Thio-substituted nucleotide analogues (dNTPαS) are expected to perturb the chemical step selectively. Use of dNTPαS results in a reduced rate for the slow fluorescence transition, while the rate of the fast transition is unperturbed.[23]

(c) When a dideoxy-terminated primer is used to eliminate the chemical step while allowing all preceding steps to occur, the rapid fluorescence transition is unaffected, while the slow fluorescence transition disappears.[18] Results (a−c) strongly support the hypothesis that the fast and slow fluorescence transitions reflect a conformational change and the chemical step, respectively.

(d) Similar to the results from (c), binding of substitution-inert Cr(III)dNTP to the Pol β·DNA binary complex induces the fast phase of the fluorescence change only.[16] Since no free metal ions are present, eliminating the catalytic metal ion binding step (step 3 in Figure 3) but allowing all preceding steps to occur, this result suggests that the fast conformational change is induced by binding of MdNTP (step 2) and precedes binding of the catalytic metal ion (step 3).

(e) The above result with Cr(III)dNTP was corroborated by use of Rh(III)dNTP (Figure 4A). Further, when Pol β is preincubated with DNA substrate + Rh(III)dCTP and the reaction is then initiated with Mg^{2+}, so that only catalytic Mg^{2+} binding and the subsequent steps can be observed, the fast fluorescence transition is absent while the slow transition is present and unaffected (Figure 4B**),**[23] indicating that the slow fluorescence transition occurs only upon binding of the catalytic magnesium ion.

(f) When the experiment described in (e) (and illustrated in Figure 4B) is run with a dideoxy-terminated primer, so that the window of observation begins with catalytic Mg^{2+} binding and ends immediately before the chemical step, no signal is observed (Figure 4C). This result suggests that the slow fluorescence transition results either from the chemical step itself or from a step thereafter. While the step directly responsible for the slow fluorescence transition may itself be rapid, it must be limited in rate by the same step which limits nucleotide incorporation (because the slow fluorescence transition and nucleotide incorporation occur at the same rate).

(g) Comparison of the Pol β pre- and postchemistry (i.e. prior to pyrophosphate release) ternary complexes reveals negligible structural changes,[18] suggesting that phosphodiester bond formation itself is not responsible for the slow fluorescence transition. We therefore hypothesized that the slow fluorescence transition corresponds to a conformational change occurring after chemistry. Note that this postchemistry conformational change would be insensitive to altered viscosity as long as a preceding step remained rate-limiting; this would explain why the slow fluorescence transition was unaffected by increased viscosity above in experiment (a). To confirm that the event responsible for the slow fluorescence transition is not the chemical step itself, we attempted to differentially perturb the rate of chemistry and the rate of the slow fluorescence transition. By raising assay buffer pH (from 7.0 to 8.4), we increased the rate of Pol β-catalyzed single-dNTP incorporation. By concomitantly increasing the buffer viscosity (from 10% to 35% glycerol), we selectively slowed conformational steps, creating a situation in which the rate of dNTP incorporation (determined by rapid quench) is faster than the rate of the second fluorescence change in stopped-flow (Figure 4D).[24] This dissection of the rate of chemistry and the rate of the slow fluorescence change is consistent with our suggestion that the slow fluorescence change reflects a conformational step *after* chemistry (most likely subdomain reopening).

2.4. Confirmation of Results from Rh(III)dNTP without Using Analogues

While use of various analogues (e.g., dideoxy-terminated primers, dNTPαS, and substitution-inert metal·nucleotide complexes) has made it possible to dissect microscopic steps and to characterize the structures of intermediates, it is conceivable that these analogues cause unexpected or unknown perturbations to the reaction mechanism. Thus, when the experimental properties of Pol β are shown to be different from those of other polymerases or different from results of computational studies with Pol β, the use of analogues is often cited as the cause of the discrepancy.[25] One way to address this issue is to employ multiple, different analogues. If the results and interpretations for a variety of analogues are consistent, as described in the previous section, then the danger of misinterpretation owing to an analogue-introduced artifact is diminished. However, the best method to eliminate the possibility of an analogue-introduced artifact is to simply employ an experimental condition that utilizes only natural substrates but which achieves the same effect conferred by the analogue. To this end, we modulated Mg^{2+} concentrations to achieve the same effect conferred by Cr-

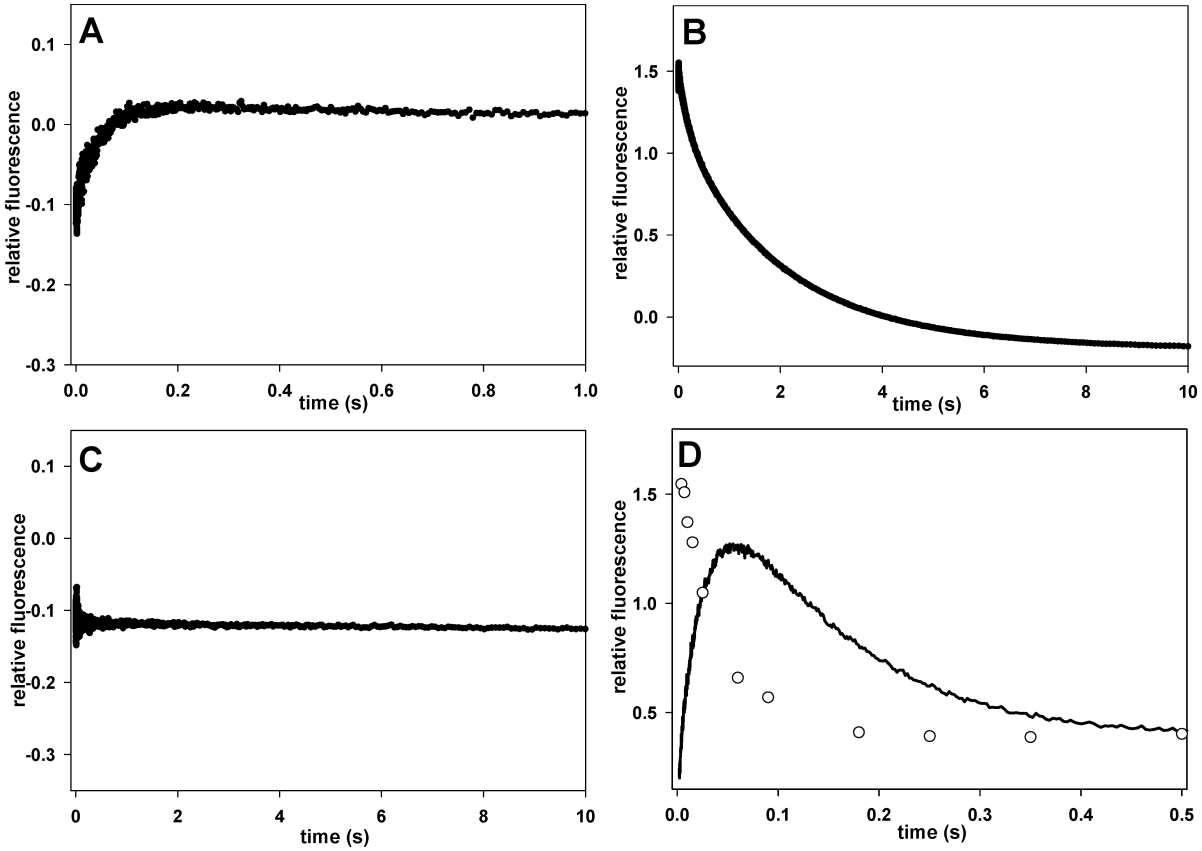

Figure 4. (A) Stopped-flow 2AP fluorescence assay monitoring Rh(III)dCTP binding to the Pol β·DNA binary complex (DNA substrate was 35mer/18mer template/primer with a nascent templating guanine). (B) Stopped-flow 2AP fluorescence assay monitoring single-nucleotide incorporation upon addition of Mg^{2+} to the *preassembled* Pol β·DNA·Rh(III)dCTP ternary complex described in part A. (C) Similar to the assay in part B, except a dideoxy-terminated primer was used. (D) Rapid quench (○) and 2AP fluorescence stopped-flow (—) assays monitoring Pol β-catalyzed single-nucleotide incorporation (of dATP opposite to templating thymine in a 36mer/19mer 2AP-containing DNA substrate) under conditions of increased pH and increased buffer viscosity.[24] Parts A−C are reproduced with permission from ref 23. Copyright 2005 American Chemical Society.

(III)dNTP and Rh(III)dNTP (namely, saturation of the MgdNTP binding site while maintaining essentially no free Mg^{2+}).[23] This was accomplished by taking advantage of Pol β's different binding affinities for MgdNTP and the catalytic Mg^{2+} ($K_{d,MgdATP} = 46\ \mu M$ and $K_{d,Mg} = 1.0$ mM[21]). With dNTP in large excess of Mg^{2+}, it is possible to achieve substantial MgdNTP binding within the active site, while at the same time maintaining a free Mg^{2+} concentration that is too low to support significant occupation of the catalytic Mg^{2+} binding site.

Figure 5A shows 2AP fluorescence stopped-flow assays at varying concentrations of MgdATP and essentially no free Mg^{2+}. Under these conditions, the binding of MgdATP induces the fast fluorescence transition exclusively. Addition of excess Mg^{2+} to the preformed Pol β·DNA·MgdNTP ternary complex results in the slow fluorescence transition only (Figure 5B), analogous to what was observed upon addition of Mg^{2+} to the preformed E′·DNA·Rh(III)dNTP ternary complex in Figure 4B. That these results resemble the data obtained with both Cr(III)dTTP and Rh(III)dCTP supports the contention that the analogues have not produced artifactual stopped-flow results.

The conclusion that the nucleotide-induced conformational change is relatively rapid and that the rate-limiting step occurs after catalytic Mg^{2+} binding obviously argues that nucleotide-induced subdomain closure, the conformational change directly observed by X-ray crystallography, cannot be rate-limiting. This was indeed supported by structural analyses of some of the intermediates, as described in the next section.

2.5. Structural Support for the Kinetic Mechanism

It clearly enhances our understanding of both the kinetic and the structural mechanisms if the two can be correlated, linking structural intermediates to individual states in the kinetic pathway. Specifically, since kinetic models typically infer the existence of intermediate states and microscopic transformations through indirect analyses, such models are strengthened when the existence of these states can be corroborated by experimental structural results and when the sequence and rates of microscopic transformations appear to be consistent with directly observed structural differences.

The structures of free Pol β, its binary complex (with DNA), and its prechemistry ternary complex (with DNA, MgdNTP, and catalytic Mg^{2+}) were solved by X-ray crystallography early on[14,26,27] and are reviewed in another article of this issue.[1] In this section we describe additional structural studies that provide support for the kinetic mechanism described above in section 2.3. As background, it is only important to know that Pol β displays a canonical polymerase architecture consisting of thumb, palm, and fingers subdomains, and also has an additional N-terminal 8-kDa domain (Figure 6). The thumb subdomain (along with the 8-kD domain) is extensively involved in DNA binding and displays a modest backbone conformational change upon formation of the binary complex. The fingers subdomain is significantly

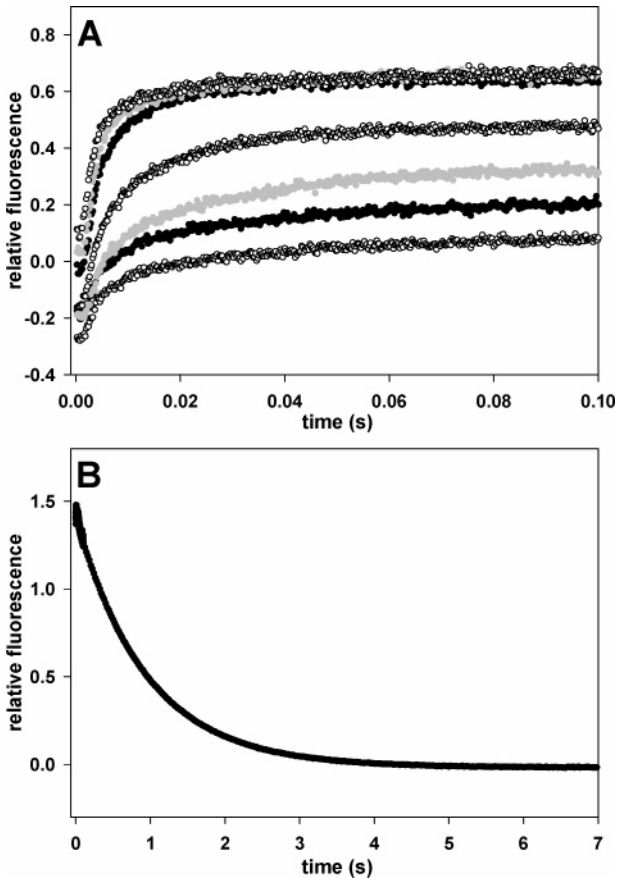

Figure 5. (A) Stopped-flow 2AP fluorescence assays monitoring Mg(II)dATP binding to the Pol β·DNA binary complex (where the DNA substrate was a 36mer/19mer template/primer containing a nascent templating thymine). Syringe 1 contained the Pol β·DNA binary complex in assay buffer containing 1 mM EDTA. Syringe 2 contained assay buffer with 2 mM dATP, 1 mM EDTA, and varying concentrations of $MgCl_2$. The calculated postmixing concentrations of the MgdATP complex are (from bottom to top): 1.3, 3.1, 9.8, 25, 67, 122, and 270 μM. (B) Three-syringe sequential mixing stopped-flow experiment monitoring addition of Mg^{2+} to the preformed E′·DNA·MgdATP ternary complex. The "priming" phase of the reaction was conducted as described above for part A, using a saturating concentration of MgdATP. After a delay of 150 ms, the preassembled ternary complex was mixed rapidly with a third solution containing 22 mM $MgCl_2$ in assay buffer, and 2AP fluorescence was monitored. Parts A and B are reproduced with permission from ref 23. Copyright 2005 American Chemical Society.

involved in MgdNTP binding and changes conformation modestly upon progression from the binary to the ternary complex; note, however, that the first structure of the ternary complex to be solved was thought to contain both MgdNTP and the catalytic Mg^{2+}, and it was not known whether both of these were required to induce repositioning of the fingers subdomain. Although the palm subdomain contains the catalytic aspartate triad—which is intimately involved in binding both MgdNTP and the catalytic Mg^{2+}—it does not display substantial backbone conformational changes upon binding of these ligands (Figure 6).

In 2001 Arndt *et al.*[18] determined the structure of an intermediate ternary complex containing DNA and MdNTP but no catalytic Mg^{2+}: the Pol β·DNA·chromium(III)2′-deoxythymidine-5′-β,γ-methylene-triphosphate (dTMPPCP) complex (Figure 7A). In addition to not having the catalytic Mg^{2+} ion bound, this complex differed from all previous polymerase·DNA·MgdNTP complexes in that the primer was

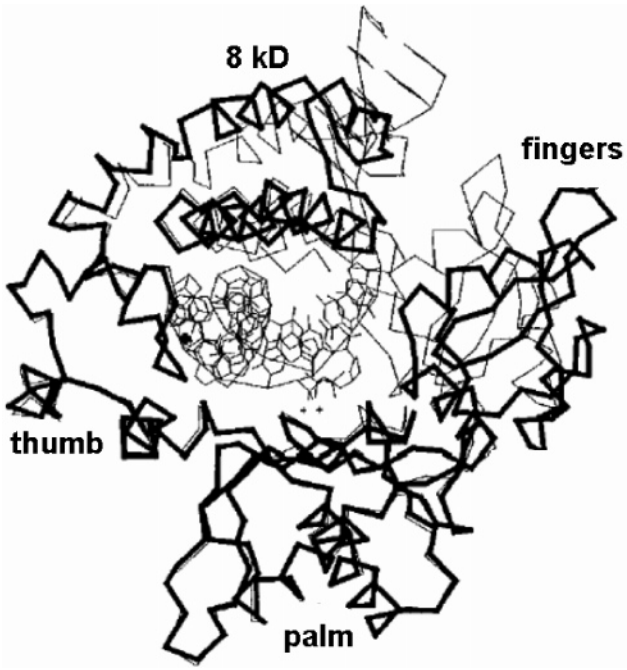

Figure 6. α-Carbon traces comparing the subdomain positioning of Pol β in the open binary (thick lines) and closed ternary (thin lines) complexes. Note that the fingers, palm, and thumb subdomains are labeled according to the notation of Steitz.[121] Adapted with permission from ref 14.

not dideoxy-terminated, making it a fully functional intermediate structure. This was confirmed by the fact that soaking the ternary complex crystal in Mn^{2+} solution (which was used in lieu of Mg^{2+} because of its greater electron density) resulted in crystal transformation to the product complex [Pol β·DNA·Cr(III)PCP]—the structure of which was also determined (Figure 7B). The critical feature of the prechemistry ternary complex was that the fingers subdomain was closed, with backbone conformation virtually identical to that of previous Pol β ternary complexes containing bound catalytic Mg^{2+} ion (Figure 7C). This structural result confirmed that the fingers subdomain closure, which had been observed in previous prechemistry ternary complexes, is induced specifically and exclusively by binding of MdNTP, with no requirement for, or contribution from, the catalytic metal ion.

Ideally, high-resolution structures would be available for each intermediate ground-state in the reaction pathway, in addition to the ternary complex containing a transition-state analogue for the chemical step. Moreover, a rigorous understanding of the structural determinants of fidelity would require complementary structures for mismatch incorporation. In reality it is not feasible to solve all of these structures by X-ray crystallography. As complementary approaches, nuclear magnetic resonance (NMR) and small-angle X-ray scattering (SAXS) can provide information about the conformational state of the enzyme at each intermediate step. Although the size of DNA polymerases is at the high-end limit of NMR, promising results have been obtained for Pol β.[28,29a] Additionally, we recently demonstrated the efficacy of SAXS for monitoring different conformational states along Pol β's reaction pathway: distinct profiles are observed for the free enzyme, the E·DNA binary complex, and the E′·DNA·MgdNTP ternary complex (Figure 8).[29a] The value of this high-throughput technique is illustrated in the following example. A critical question related to polymerase fidelity

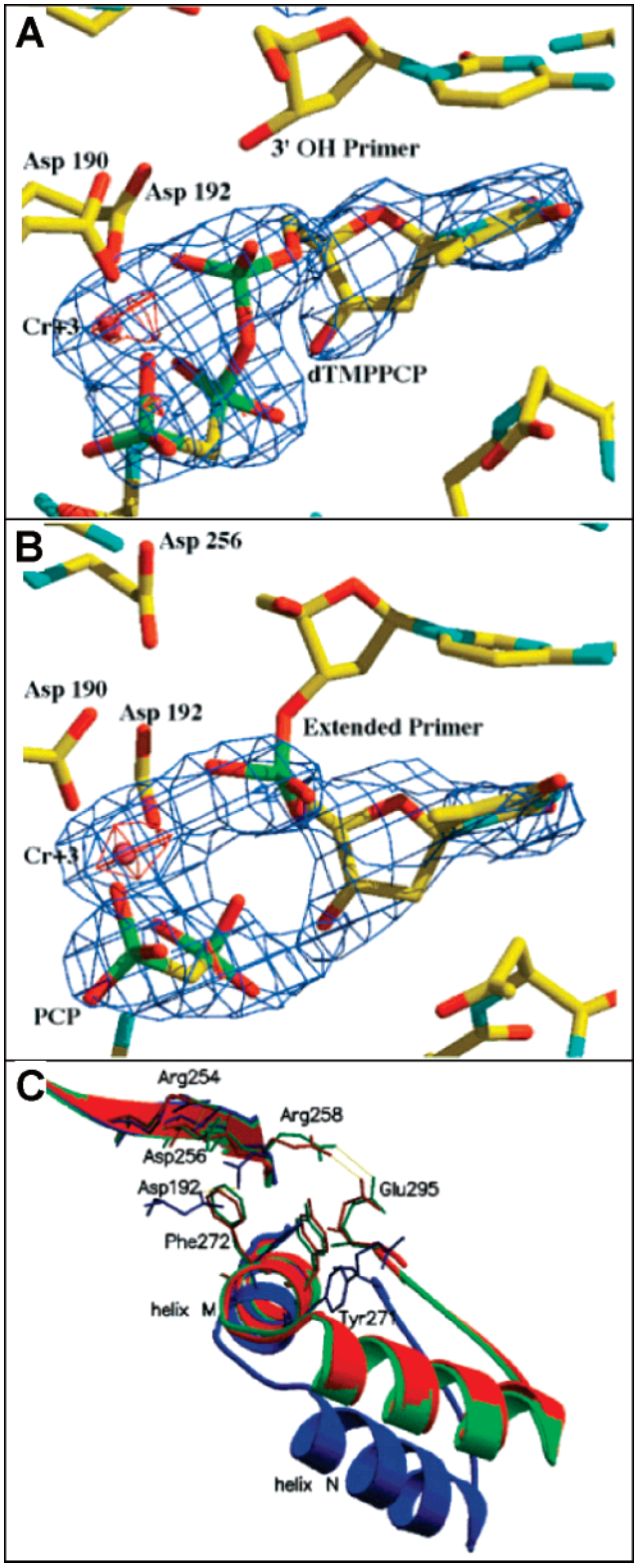

Figure 7. Crystal structures of Pol β reaction intermediates. (A) The prechemistry Pol β·DNA·Cr(III)dTMPPCP ternary complex showing the presence of the nucleotide-associated Cr^{3+} ion and the absence of the catalytic metal ion (1XUO). (B) The postchemistry Pol β·DNA·Cr(III)PCP complex (1XUZ). (C) Comparison of the open conformation Pol β·DNA binary complex (blue) (1BPX) with the closed conformation Pol β·DNA·Cr(III)dTMPPCP ternary complex (red) and the closed conformation Pol β·DNA·Mg_2ddCTP ternary complex [with two metal ions bound (green) (1BPY)]. Reproduced with permission from ref 18. Copyright 2001 American Chemical Society.

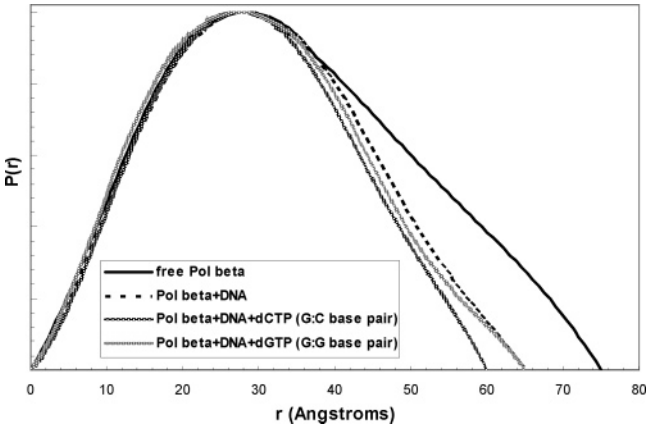

Figure 8. SAXS $P(r)$ plots comparing free Pol β, the Pol β·DNA binary complex, and the Pol β G:C and G:G ternary complexes. The sample consists of 0.2 mM Pol β, 10 mM $MgCl_2$, 10 mM dithiothreitol, 50 mM phosphate buffer (pH 8.0), and 0.15 M KCl. Gapped DNA (0.2 mM) and additional 10 mM dNTP were added to form the complexes. SAXS experiments were conducted on beamline 4-2 at the Stanford Synchrotron Radiation Laboratory. Data were collected at a wavelength of 1.3776 Å and a sample-to-detector distance of 1.5 m, at 20 °C. The program GNOM[29b] was used to determine $P(r)$ from the measured scattering intensity $I(q)$. $P(r)$ is the distribution of interparticle vector lengths within a single scattering particle. From $P(r)$, d_{max}, the maximum linear dimension of the particle, and R_g, the average distance from the center of a particle to scattering segments within that particle, can be determined. Details will be described in ref 29a.

is whether an incorrect incoming dNTP is discriminated against simply because it inefficiently induces the canonical open-to-closed conformational change or whether, alternatively, it forces the enzyme to proceed along a different conformational pathway.[3,30−32] SAXS profiles (Figure 8) and ^{15}N-HSQC NMR (not shown) of Pol β indicate that the properties of the G:G ternary complex fall between those of the G:C ternary complex and the E·DNA binary complex. It is expected that additional studies using both NMR and SAXS will be able to shed further light on Pol β's mechanism of fidelity.

2.6. Evidence for Fast Conformational Change from Other Studies

In parallel to our kinetic and structural studies, the fast subdomain closure in Pol β has been reported by other groups using a variety of approaches. (i) Site-directed mutagenesis and pre-steady-state kinetic analysis of Pol β indicated that valine substitution for aspartate 276 in the fingers subdomain decreased the $K_{d,app}$ for the incoming nucleotide. Since interaction between Asp276 and the nascent base pair is observed only in the closed conformation of Pol β, the result suggests that "the subsequent rate-limiting conformational change is not the open-to-closed structural transition".[33] (ii) To specifically probe the dynamics of the fingers subdomain, the single native tryptophan of Pol β was replaced with alanine, while tryptophan was strategically substituted for leucine in the fingers subdomain. Analysis of the dynamics of tryptophan fluorescence anisotropy decay for this mutant indicated that fingers segmental motion is far more rapid than the step limiting single-nucleotide incorporation.[34] (iii) A recent computational study also suggests that the rate-limiting step in Pol β conformational closing is not identical to the rate of nucleotide incorporation and that the rate-limiting step in both correct and incorrect nucleotide

incorporation occurs after the subdomain closing conformational change.[32]

Taken together, the Pol β field has now reached a consensus that the open-to-closed conformational change induced by MgdNTP (step 2 in Figure 3) is a fast, non-rate-limiting step. This does not mean that this step cannot differentiate correct and incorrect dNTP, only that it is not likely to be a major dictator of fidelity, as further elaborated in the next section. On the other hand, our conclusion that the chemical step is rate-limiting and thus the main determinant of fidelity for Pol β has not yet received corroboration from other labs. As we have pointed out,[23] the chemical step can be further dissected into multiple microscopic steps with different rates by use of different experimental or computational techniques at different time scales. A recent computational study suggested that after subdomain closing and catalytic Mg^{2+} binding, but prior to chemistry, a localized reorganization of active site architecture is required and may be rate-limiting.[35] As also indicated by the authors, from the perspective of the kinetic mechanism, it is not clear whether such local repositioning preceding chemistry should be regarded as distinct from the chemical step.

2.7. Mechanism of Fidelity for the DNA-Repairing Enzyme Pol β

At the most direct level, a polymerase's fidelity obviously results from the free energy difference between the most unstable transition-states in the reaction pathways for correct and incorrect nucleotide incorporation. Regardless of whether one takes the view that the free energy of the rate-limiting transition-state is "caused by" the free energies of the preceding or following steps, complete understanding of the mechanism of fidelity, from the kinetic standpoint, requires determination of the free energy profiles (or microscopic rate constants for each step) for the correct and incorrect nucleotide incorporation reactions. From the structural standpoint, the structures of at least all ground-state species for both correct and mismatched nucleotide incorporations and, ideally, a structure of the complex bound to a transition-state analogue for the chemical step would be necessary. In addition to this copious amount of information, complete understanding of the mechanism of polymerase fidelity would require that all the same information be known for the corresponding *non-enzyme-catalyzed reactions*. For example, even the magnitude of fidelity that the enzyme confers upon the reaction cannot truly be understood without knowing what the selectivity of the non-enzyme-catalyzed reaction is. However, such information may be experimentally unobtainable due to the high free energy barriers associated with these reactions, and thus, the free energy of ground-state base-pairing is frequently used as an approximation.

While the currently available data are very incomplete relative to the imposing list above, substantial progress has been made in several key areas, particularly in identification of the rate-limiting step, determination of relative rates for other steps, and determination of structures of a number of intermediate states. This is all best established for (enzyme-catalyzed) correct nucleotide incorporation, but some progress has been made for incorrect nucleotide incorporation as well. Figure 3B shows qualitative free energy profiles for correct and incorrect nucleotide incorporation according to the results described above. Note that complete and experimentally derived free energy profiles have previously been constructed for other polymerases;[11,36] however, these profiles relied heavily on thio-effect data, which is considered by many researchers to have a high propensity to mislead.[19,37,38]

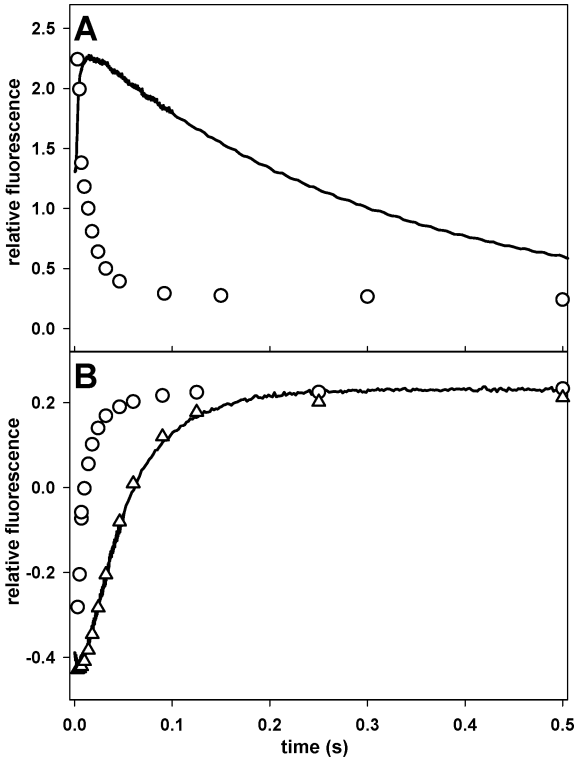

Figure 9. (A) Comparison of KF rapid quench (○) and 2AP fluorescence stopped-flow (—) time courses for single-nucleotide incorporation into a 36mer/19mer template/primer substrate. To facilitate comparison of the two data sets, the rapid quench data illustrates substrate consumption rather than product formation.[24] (B) KF catalyzed single-nucleotide incorporation into a 36mer/18mer template/primer substrate, as monitored by 2AP fluorescence. Superimposed on the fluorescence trace are data for the first (○) and second (△) nucleotide incorporation into the same 36mer/18mer substrate, as monitored by rapid quench.[24]

2.8. Is the Mechanism of Pol β an Anomaly?

Since our conclusion that chemistry is the rate-limiting step for Pol β differs from earlier conclusions (based largely on results for other polymerases) that the fingers subdomain closing conformational change is rate-limiting, it is important to consider whether a common rate-limiting step is shared by most polymerases and whether Pol β represents an exception to this rule, as suggested recently.[3] Kinetic similarity to Pol β has already been observed in at least three cases. First, direct monitoring of fingers subdomain motions in Klentaq1, using fluorescence resonance energy transfer, indicated that subdomain closing is substantially faster than the rate of single-nucleotide incorporation.[39] Second, we have undertaken stopped-flow analyses of KF in parallel with Pol β.[24] During single-nucleotide incorporation KF displays a biphasic fluorescence change (Figure 9A, solid curve), where the rate of the first fluorescence transition is faster than the rate of nucleotide incorporation (as measured by rapid-quench). Analogous to the case of Pol β, use of a dideoxy-terminated primer abolishes the second fluorescence transition while leaving the first fluorescence transition unperturbed. However, unlike the case of Pol β, the rate of KF-catalyzed single-nucleotide incorporation (Figure 9A, circles) is faster than the rate of the second fluorescence change. To examine the nature of the step responsible for the slow fluorescence

change during single-nucleotide incorporation by KF, we performed a two-nucleotide incorporation rapid quench assay using the same substrate employed in the stopped-flow assay (Figure 9B). We found that (a) incorporation of the second dNTP is significantly slower than that of the first dNTP and (b) incorporation of the second dNTP occurs at a rate similar to the rate of the slow fluorescence change in the single-turnover stopped-flow assay. These results indicate that the slow phase of fluorescence change corresponds to a physical step that limits the rate of the second but not the first dNTP incorporation. Collectively, the above data led us to *hypothesize* that similar to the case of Pol β the fast and slow fluorescence changes for KF represent, respectively, subdomain closing before chemistry and subdomain reopening after chemistry; note that the latter is consistent with the findings of Dahlberg and Benkovic, who previously described a slow postchemistry conformational change in KF.[11] Third, recent computer simulations of the free energy landscape for correct and mismatched nucleotide incorporation by T4 polymerase also indicate that the chemical step (namely, P−O dissociation) is rate-limiting.[40]

Though both experimental and computational data are consistent with the model that chemistry is the rate-limiting step *through phosphodiester bond formation* for some polymerases (Pol β, KF, Klentaq1, and T4 pol), it would be too simplistic to invoke a common rate-limiting step for all members of this class of enzymes. Importantly, stopped-flow results for Pol β suggest that fingers subdomain closure is faster than chemistry by a factor of 100 at pH 7.0 and by less than a factor of 10 at pH 8.0, while the two steps approach equality in rate above pH 8.8; this demonstrates that the relative rates of microscopic steps can vary as a function of assay conditions, a fact which can be important both during kinetic analyses of an individual enzyme and when attempting to make comparisons between different enzymes.

3. Mammalian Error-Prone DNA Polymerases

3.1. Background

The general belief that DNA polymerases should follow, and even accentuate, the Watson−Crick base-pairing rules during replication and repair of DNA has been challenged in recent years by the discovery of highly error-prone polymerases within each of the three kingdoms of life.[41] The defining characteristic of a low-fidelity polymerase is of course the propensity to incorporate non-Watson−Crick base-paired nucleotides into a growing DNA strand with relatively high frequency. While there is not an exact line that separates low and high fidelity, it could perhaps be said that high fidelity is above 10^4-10^5 and low fidelity is below 10^3. Many low-fidelity polymerases also have the ability to catalyze nucleotide incorporation opposite to, or downstream of, templating nucleotides that are chemically damaged (hence the designation "translesion polymerase") with unusually high efficiency.[7,42] These unique capacities, depending on the context in which they are employed, can serve two purposes. First, by synthesizing past lesions that would otherwise block the replisome, translesion polymerases can promote survival by facilitating completion of replication. Second, by replicating DNA with a very high error frequency, low-fidelity polymerases can promote genetic variability. Seven error-prone DNA polymerases, belonging to three different polymerase families, have been identified in humans;[5,6] a different biological function has been proposed for each of these, though at varying levels of detail.

Pol ζ is the only known low-fidelity member of the B polymerase family, a family which also includes high-fidelity, replicative enzymes. On the basis of Pol ζ's unique ability to efficiently extend a mismatched primer terminus (in which the nascent base pair contains a damaged templating nucleotide), it is thought that the enzyme plays a role in rescuing such mismatched termini from being replicative dead-ends.[42−44]

Pol λ and Pol μ are human low-fidelity members of the X-family, the same family to which Pol β and ASFV Pol X belong. Indeed, Pol λ is closely homologous to Pol β, yet it is 10- to 100-fold more error-prone.[45] Pol μ is homologous to terminal deoxynucleotidyltransferase, a template-independent polymerase, and while Pol μ is capable of template-independent synthesis, it appears to be more efficient incorporating nucleotides opposite a template, albeit with low fidelity. A biological function has not been proposed in great detail for either of these low-fidelity enzymes, although it has been suggested that they may play roles in homologous chromosome recombination during meiosis, double-strand break repair, and/or somatic hypermutation.[6]

The remaining four low-fidelity human polymerases, Rev1 and Pol's ι, η, and κ belong to the Y-family, and indeed every known member of this family, from any source, is low-fidelity, and most are competent in translesional synthesis. Each of these polymerases, while quite error-prone on undamaged DNA, has high base pair specificity in at least one instance, usually opposite damaged DNA.[46−51] Accordingly, Pol κ is able to bypass benzo[*a*]pyrene with unusual efficiency and accuracy, by inserting the correct dCMP opposite the lesion.[52] Pol η efficiently and accurately incorporates two dAMP's opposite thymidine−thymidine cis−syn dimers, UV-induced lesions which severely inhibit most polymerases.[47] It is possible that human Pol η is involved in error-free bypass of other DNA lesions as well, given that the highly homologous yeast Pol η accurately and efficiently incorporates dCTP opposite 8-oxoG.[53] Pol ι and Rev1 have both been suggested to be involved in error-free bypass of α-OH-PdG, inserting correct dCTP opposite the lesion.[49] Pol ι has also been suggested to be involved in the repair of A:U and G:T base pairs (the latter resulting from 5-methylcytosine deamination), which can explain its remarkable selectivity for A:T base pair formation, and against T:A base pair formation.[54] In general, the major biological function of Y-family polymerases is thought to be error-free repair of otherwise replication-inhibiting sites of DNA damage, although, as for the case of the low-fidelity mammalian X-family polymerases, it is thought that there may be a role in somatic hypermutation as well.[6]

3.2. Kinetic Mechanism of Error-Prone DNA Polymerases

Several eukaryotic error-prone polymerases have been characterized kinetically in steady-state and pre-steady-state studies.[45,46,50,51,55−58] Pol η is the first Y-family polymerase for which a detailed kinetic analysis was performed,[59] and it remains one of the best characterized error-prone polymerases.[47,53,57,60−64] Pre-steady-state kinetic analyses of yeast and human Pol η[57,59] show that while the two enzymes generally have comparable $k_{pol}/K_{d,app}$ values for both correct and incorrect nucleotide incorporation, the human enzyme tends to have larger k_{pol} and $K_{d,app}$ values, for both incorpora-

tion types, than does the yeast enzyme. For example, typical $K_{d,app}$ values for human Pol η are 110 and 380 μM, for correct and incorrect incorporations, respectively, whereas typical values for yeast Pol η are 2.5 and 13 μM, respectively. On this basis, it was concluded that the yeast polymerase makes more contacts with the incoming nucleotide during the initial binding step and that ground-state binding interactions make a greater contribution to fidelity for yeast Pol η than for human Pol η.[57,59] While it should be remembered that $K_{d,app}$ values cannot necessarily be correlated directly and exclusively with initial ground-state binding, it is nonetheless clear from these results that, while the two homologous enzymes have a comparable sum of binding interactions for the rate-limiting transition-state, a greater proportion of those interactions are realized earlier in the reaction pathway for the yeast enzyme and later in the reaction pathway for the human homologue. Note that, based on a small thio-effect and on pulse-chase experiments, it was proposed that a conformational change step, rather than chemistry, is rate-limiting for both correct and incorrect nucleotide incorporations.[57,59] The pulse-chase experiment showed that ~13% of "pulsed" radioactive nucleotide proceeds through chemistry when "chased" with an abundance of nonradioactive nucleotide, interpreted to indicate that at least this proportion of the complex exists in a slowly exchanging closed complex when the chase is introduced.[59] These observations led the authors to the conclusion that, similar to what has been proposed for a number of high fidelity polymerases, Pol η utilizes a rate-limiting, "induced-fit" conformational change to enhance its ability to select the desired substrate. In addition, the use of nucleotide analogues that are not able to form hydrogen bonds suggests Watson−Crick hydrogen bonds make an important contribution to Watson−Crick base pair selectivity.[63] A hydrogen bond between the enzyme and the incoming dNTP is also thought to make a significant contribution, but there is no corresponding interaction between the enzyme and the templating base.[62]

Pol ι is another human polymerase with unique properties. While most DNA polymerases have similar catalytic efficiencies for the four Watson−Crick base pairs, Pol ι discriminates very strongly between Watson−Crick base pairs, with catalytic efficiencies that vary tremendously depending on the templating base.[50,58] For example, A:T base pair formation has a catalytic efficiency 200-times greater than that of T:A formation. While T:A formation is unusually inefficient, even by low-fidelity polymerase standards, efficiency for A:T formation is comparable to that of high-fidelity polymerases. As a result of this, Pol ι demonstrates fairly high fidelity for incorporation opposite a templating A, whereas fidelity opposite a templating T is exceptionally low. For example, catalytic efficiency for formation of mismatched T:G is more than 10-fold greater than that for Watson−Crick T:A formation. This particular instance of infidelity results almost entirely from $K_{d,app}$ differences, with $K_{d,app}$ 10-fold higher for T:A formation than for mismatched T:G formation. Thus, once again, the binding interactions which favor mismatch incorporation are realized early in the reaction pathway.

Extensive pre-steady-state studies have also been performed with Dpo4 polymerase, an archael homologue of mammalian Pol κ,[65,66] and one of the less error-prone of the low-fidelity polymerases. Similar to high-fidelity enzymes, Dpo4 has k_{pol} values ~2−3 orders of magnitude greater for Watson−Crick base pair formation than for mismatched base pair formation. Unlike high-fidelity enzymes, however, Dpo4 has comparable $K_{d,app}$ values for Watson−Crick base-paired and mismatched dNTP's. Thus, little to no distinction is made early in the reaction pathway, and modest distinction arises only on the approach to the rate-limiting step. In the case of Dpo4, thio-effect and pulse-chase results formed the basis for the proposal that chemistry is not rate-limiting for correct dNTP incorporation but that it may be for incorrect dNTP incorporation,[65] as has previously been suggested for a number of high-fidelity polymerases.

Pre-steady-state studies of a truncated form of human pol λ likewise showed that minimal nucleotide distinction exists at the level of $K_{d,app}$ (with values ranging from 1 to 8 μM for both correct and incorrect dNTP incorporation).[45] On this basis, it was suggested that Pol λ cannot differentiate match and mismatch nucleotides during initial ground-state binding and that the rate of nucleotide incorporation makes the dominant contribution to Pol λ fidelity.

In contrast to the above, Pol μ, another X-family polymerase, makes significant distinction in favor of Watson−Crick base-paired dNTP incorporation at the level of $K_{d,app}$,[55] with values of 0.35−1.8 and 7.3−135 μM for correct and incorrect dNTP, respectively. However, with fidelity values ranging from 10^4 to 10^5 (comparable to Pol β), Pol μ is not a low-fidelity enzyme in terms of nucleotide selectivity. Rather, Pol μ makes frame-shift errors at a high rate,[67] and thus, it is doubtful whether its mechanism of infidelity can be directly related to those enzymes which have low nucleotide incorporation fidelity.

In summary, the picture of the mechanism of fidelity (or of infidelity) of low-fidelity polymerases is far from complete; however, catalytic efficiency measurements have been made for correct and incorrect nucleotide incorporations for a number of these enzymes, and two important trends emerge. First, as has been noted previously,[68] low-fidelity tends to result not from enhanced catalytic efficiency for misincorporation (relative to high-fidelity enzymes) but rather from attenuated catalytic efficiency for Watson−Crick incorporations, resulting in low overall catalytic efficiency and low fidelity. Second, low-fidelity polymerases tend to exhibit their low fidelity in the $K_{d,app}$ parameter rather than in the k_{pol} parameter. This has frequently led to the conclusion that such an enzyme makes minimal distinction, or favors the mismatched dNTP, during initial ground-state binding. It is important to note once again, however, that, to whatever extent the identity of the rate-limiting step is uncertain, $K_{d,app}$ cannot with certainty be correlated to initial dNTP binding. In particular, if the rate-limiting step does not immediately follow initial binding, then intervening ground-states can have a substantial impact on $K_{d,app}$. Significantly, a number of thio-effect and pulse-chase studies of low-fidelity polymerases have suggested that a conformational change, which may immediately follow dNTP binding, is rate-limiting. As we have argued above though, such studies have the capacity to mislead,[19] and more direct means exist to probe this important question. In any case, it is possible to conclude that low-fidelity polymerases tend to realize binding interactions which are nondiscriminatory, or which favor a mismatched dNTP, early in the reaction pathway, and they tend to realize interactions which favor a Watson−Crick base-paired dNTP later in the reaction pathway.

3.3. Structures of Error-Prone DNA Polymerases

A substantial number of crystal structures of error-prone polymerases, free and in complex with different substrates,

have been solved in the past 5 years.[69−79] These enzymes, all from the X- and Y-families, possess negligible sequence homology to other polymerase families but generally have the canonical polymerase architecture consisting of fingers, palm, and thumb subdomains. In addition, crystal structures of Y-family polymerases reveal the presence of an additional subdomain, termed the "little finger", which possesses a high degree of sequence diversity between Y-family members. The little finger appears to be involved in DNA binding and is believed to play an important role in determining and conferring the unique low-fidelity properties of these enzymes.[80]

One theory for the structural origin of low-fidelity DNA polymerization is that error-prone enzymes possess relatively loose, solvent accessible active sites that are able to accommodate "differently shaped" mismatched base pairs, as well as damaged or chemically modified base pairs.This theory is supported by a number of structural studies. For example, the ternary complex of Dpo4[72] reveals a relative paucity of interactions between the enzyme and the nascent base pair. Specifically, the fingers subdomain, which makes numerous interactions with the nascent base pair in many high-fidelity enzymes, is relatively small in Dpo4 and makes few such contacts. Those residues which do interact at or near the nascent base pair have small side chains, as opposed to high-fidelity enzymes which frequently employ aromatic stacking interactions with the bases and electrostatic interactions with the backbone. This results in a Dpo4 active site which leaves the nascent base pair relatively unrestrained, with a greater allowance for wobble base pairs and bulky adducts. In contrast to this, however, a modeled structure of the catalytic core of the homologous human Pol κ suggests that it interacts strongly with the templating base.[78]

The structure of the catalytic core of human Pol λ in three intermediate states has been solved: a binary complex with gapped DNA, a prechemistry ternary complex with DNA and incoming dNTP, and a postchemistry ternary complex with extended DNA and PP_i.[69,70] The binary complex structure indicates that Pol λ makes limited contacts with the DNA duplex, interacting with only the first two base pairs upstream of the primer terminus, although there are several interactions with the DNA downstream of the gap.[69] Of particular interest, unlike the cases of a number of high-fidelity enzymes, the interactions which Pol λ has with the upstream segment of the DNA do not involve the DNA bases but instead are relatively nonspecific interactions with the backbone (although the prechemistry ternary complex structure reveals that dNTP binding occurs with a DNA shift that adds several base-specific interactions with the template) (Figure 10).[70] If it is indeed true that low-fidelity polymerases generally have relatively few interactions with substrates in various intermediate states, particularly around the nascent base pair, it can perhaps be inferred that there are also relatively few stabilizing interactions at the rate-limiting transition-state, which would be consistent with both the low activity and the low fidelity of these enzymes.

Another explanation for low-fidelity synthesis which has received support from structural studies is that low-fidelity polymerases do not undergo the nucleotide-induced subdomain closing conformational change that is thought to be common to all high-fidelity enzymes, and therefore, they do not benefit from the commonly invoked induced-fit selectivity enhancement. For example, comparison of the Pol λ binary and ternary complex structures indicates that Pol λ

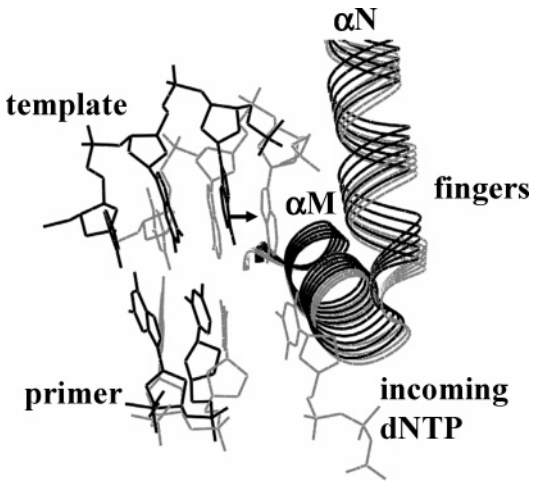

Figure 10. DNA shift induced by dNTP binding in the ternary complex of Pol λ. A portion of the DNA substrate and part of the fingers subdomain are shown for both the binary complex (PDB code: 1XSL, black) and the ternary complex (PDB code: 1XSN, gray).[70] The arrow indicates the template strand shift induced by dNTP binding in the ternary complex.

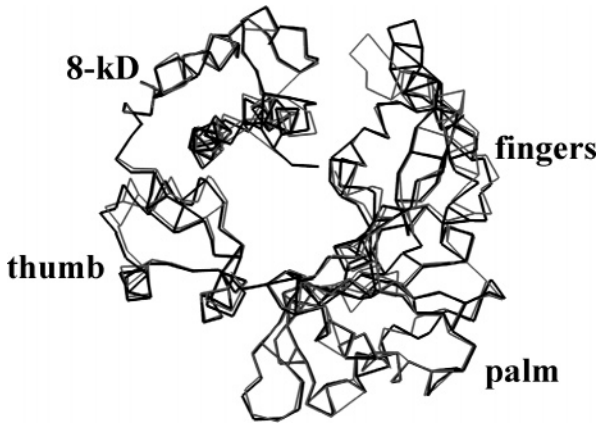

Figure 11. Superimposition of Pol λ structures: α-carbon traces of the binary (black, 1XSL) and ternary (light gray, 1XSN)[70] complexes. Both structures resemble the closed conformation of Pol β (see Figure 6), suggesting the absence of the major conformation change involving closing of the fingers subdomain, though there are local changes involving β-sheets.

exists in a closed conformation prior to dNTP binding and therefore does not undergo the dNTP-induced subdomain closure common to Pol β and all other high-fidelity enzymes for which the relevant structural information exists (Figure 11).[69,70] Similarly, the fingers subdomain of DinB appears to be in the same closed conformation when not bound to any substrate.[79] It is important to note that any conclusion that low-fidelity DNA polymerases in general do not undergo a substrate-induced conformational change is in apparent opposition to the conclusion, based on thio-effect and pulse-chase results, that several of these enzymes have rate-limiting conformational changes. One possible resolution to this potential conflict is that some low-fidelity enzymes have rate-limiting conformational changes and some have no substrate-induced conformational change. We have argued previously that polymerases in general do not have rate-limiting conformational changes and that subdomain closure exists to allow relatively rapid interconversion between a binding form which is accessible to solvent and a catalytic form which surrounds the substrate on all sides.[19] Accordingly, if some low-fidelity enzymes have active sites that are so

"loose" that they are accessible to solvent even in the catalytic state, such interconversion would apparently be unnecessary.

The active-site structures of some low-fidelity polymerases can be interpreted in terms of redirected specificity rather than reduced specificity. This would be most obviously likely for those enzymes that have low-fidelity on undamaged DNA but unusually high catalytic efficiency opposite a particular type of DNA lesion. For example, the structure of uncomplexed yeast Pol η[76] is suggestive of an active site which is relatively open, but this likely reflects an adaptation geared specifically toward accommodating bulky thymidine−thymidine cis−syn dimers rather than a nonspecific loosening. The complexed structure of human Pol ι[75] suggests that its active site stabilizes Hoogsteen base-pairing, providing a structural explanation for its accommodation of bulky templating lesions[81] as well as its enormous preference for A:T and against T:A: when held in the syn conformation, templating A can only form a base pair (that is roughly isosteric to Watson−Crick base pairs) with incoming T, whereas when templating T is forced to adopt a syn conformation, it has no viable base-pairing partner. These findings highlight Pol ι as an example of redirected, rather than relaxed, specificity.

4. Error-Prone DNA Polymerase X from African Swine Fever Virus

4.1. Background

Upon sequencing of the ASFV genome, Pol X was identified as a diminutive homologue of Pol β, projecting to a mere 20 kD.[82] As the only known low-fidelity polymerase of viral origin, the biological function(s) of Pol X may be significantly different from those of other error-prone polymerases. In this section we (a) discuss the unique fidelity/substrate specificity of Pol X, (b) attempt to correlate the kinetic properties of Pol X with its atypical structure, and (c) discuss, and present data in support of, our hypothesis that the biological role of Pol X is to introduce base substitutions via an error-prone/error-tolerant DNA "repair" pathway.

4.2. Fidelity of ASFV Pol X

Pre-steady-state kinetic constants were determined for Pol X-catalyzed formation of all 16 possible base pairs in the context of a single-nucleotide gap, revealing extreme infidelity and some very unique kinetic characteristics (Figure 12A). Perhaps the most salient feature of Pol X catalysis, apparent from the substrate specificity profile, is its comparable catalytic efficiency for formation of five base pairs, the four Watson−Crick pairs plus the G:G mismatch. Whereas all other low-fidelity polymerases are selective for one or two base pairs (e.g. A:T in the case of Pol ι, or a chemically damaged base pair in the case of several others), Pol X is the only known error-prone polymerase with such broad substrate specificity.

The unique features of Pol X catalysis that underlie its very low fidelity and its novel five base pair specificity are as follows. First, relative to Watson−Crick base-paired dNTPs, Pol X has substantially lower $K_{d,app}$ values for several mismatched incoming dNTPs. For example, $K_{d,app}$ values for dGTP in the A:G and G:G mispairs are 20 and 35 μM respectively, whereas the most tightly bound Watson−Crick

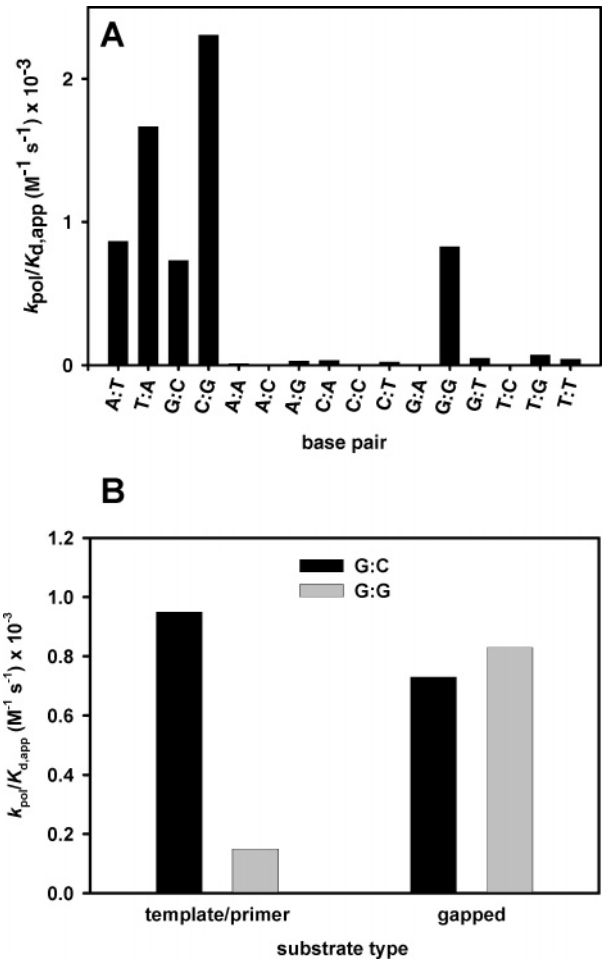

Figure 12. (A) Catalytic efficiencies for Pol X synthesis of all 16 possible base pair combinations in the context of a single-nucleotide gap. Base pairs are described by the notation X:Y, where X is the templating nucleotide and Y is the nucleotide being incorporated. (B) Comparison of Pol X-catalyzed G:C and G:G synthesis on single-nucleotide gapped and template/primer DNA substrates. Adapted with permission from ref 89.

base-paired dNTP's display ~10-fold higher $K_{d,app}$. Second, Pol X disfavors dCTP incorporation and favors dGTP incorporation regardless of the identity of the templating nucleotide. For example, C:G is the most efficiently formed Watson−Crick base pair and G:C is the least. Among the mismatches, X:G is formed the most efficiently for every applicable templating base, and X:C is formed the least efficiently for every applicable templating base. These factors converge to yield the extremely low fidelity for G:G mismatch synthesis. Despite its catalytic uniqueness, Pol X still follows the trend common to many low-fidelity polymerases: interactions which favor misincorporation are reflected principally in the $K_{d,app}$ parameter, while those which favor Watson−Crick incorporation are reflected principally in k_{pol}.

It is important to note that a recent kinetic evaluation performed in a different laboratory suggested Pol X to be a high fidelity enzyme comparable to Pol β.[83] However, the kinetic constants reported would yield half-lives for incorporation of a single nucleotide in the range of 20 min to several hours, suggesting that the activity of their enzyme is substantially lower than that used in our studies; since both labs have purified, stored, and assayed Pol X in the presence of a reducing agent, it does not seem likely that these activity

differences can be attributed to the presence/absence of Pol X's potential disulfide bond (see below). Our results have been completely reproducible in our laboratory.[84] Though we have observed some minor variation in fidelity as a result of altered reaction conditions (such as pH), the extent of variation is nowhere near the magnitude required to account for the discrepancy between the two reports.

4.3. Solution Structures by NMR

Whereas all other full-length polymerase structures, due to their size, have been determined by X-ray crystallography, the exceptionally small size of Pol X allowed it to be the first polymerase structure determined in solution by NMR (Figure 13A).[85,86] On the other hand, no crystal structure has been reported for Pol X. Consistent with what was previously predicted by modeling it to the crystal structure of Pol β, Pol X uniquely consists of only the palm and fingers subdomains out of the otherwise universal thumb/palm/fingers DNA polymerase architecture. Pol X shows overall structural homology to Pol β (Figure 13B), with particularly high homology in the active site: the carboxylate triads of the two proteins are nearly superimposable, with an rmsd of 0.90 Å for heavy atoms. However, there are a few significant differences in the structures of Pol X and Pol β. Most notably, Pol X residues 18−28 form a β-hairpin (β2 and β3), which interacts with residues 69−71 (β7) to form a three-stranded β-sheet, whereas the corresponding regions in Pol β are α-helical. This novel three-stranded β-sheet in Pol X truncates helices αA and αC relative to the homologous αJ and αL in Pol β (Figure 13A and B). Other smaller differences are found in several loop regions, with a number of loops in Pol X being shorter than the structurally homologous loops in Pol β.

Another potentially interesting structural difference between Pol X and Pol β is that Pol X has two cysteine residues, in adjacent strands (β8 and β9) of the palm subdomain, which are located close enough to one another to form an intramolecular disulfide. Of the two free Pol X structures that have been solved, one is reduced[85] and the other is oxidized.[86] This difference results in modest structural dissimilarities (Figure 13C). A kinetic analysis of the two forms indicates that (a) the published kinetic data[89] represent reduced Pol X and (b) the oxidized form is somewhat less active than the reduced form but also slightly more error-prone.[84] Which of these forms predominates *in vivo*, or whether both forms exist and what role redox interconversion may play, is not known.

Interestingly, though the thumb subdomain of Pol β is *required* for DNA binding,[87] and though crystal structures of a wide variety of polymerase complexes show the thumb to interact significantly with DNA,[26,88] Pol X binds DNA very tightly despite being thumbless; band-shift analyses indicate that Pol X binds DNA with a K_d in the low nanomolar range and slightly more tightly than does full-length Pol β.[86] How Pol X is able to achieve its affinity for DNA was elucidated by binding analyses with ^{15}N-HSQC NMR[86] and further supported by our preliminary solution structure of the Pol X ternary complex (Pol X·DNA·MgdNTP;[84] Figure 13D). Pol X uses helix αE in the fingers subdomain, helix αC in the palm subdomain, and the interface of the palm and fingers subdomains to bind DNA. The electropositive regions of these structural elements engage in an electrostatic interaction with the sugar phosphate backbone. Additionally, the hydrophobic regions on helix αE and at the interface between the palm and fingers subdomains support the bases between the duplex regions (i.e. in the single-nucleotide gap) of the DNA. This binding mode for Pol X is different from that for Pol β, as shown in Figure 13E and F.

4.4. Mechanism of the Low Fidelity of Pol X

In light of its relatively low catalytic efficiency and fidelity, one might be tempted to view Pol X as a "primitive enzyme", not yet evolved to the extent that Pol β, for example, is. Such a view would be supported by the fact that Pol X has catalytic efficiencies for Watson−Crick base pair formation that are, on average, more than 3 orders of magnitude lower than those of Pol β and also modestly lower for most mismatch incorporations.[89] However, if Pol X has evolved to catalyze controlled mutagenesis, as discussed in the next section, then low catalytic efficiency as well as low fidelity may be evolutionarily selected properties. Additionally, Pol X binds DNA as tightly as Pol β does[86] (as described above), suggesting that, at least when gauged by this property, Pol X has evolved to a comparable extent to perform its function.

It is also important to remember that the contribution a polymerase makes to fidelity can only be known by comparing enzymatic reaction rates to those of the nonenzymatic reactions, as addressed above. While the reaction rates of the non-enzyme-catalyzed reactions are not known, it seems probable, in a theoretical extension of the different free energies of ground-state Watson−Crick and mismatched base pair formation, that the mismatch incorporation reaction is intrinsically slower than the Watson−Crick incorporation—perhaps greatly so. Thus, in order for Pol X, or any low-fidelity polymerase, to have comparable catalytic efficiencies of incorporation for mismatch and Watson−Crick base-paired nucleotide incorporation, the enzyme must actually catalyze the mismatch incorporation to a greater extent—possibly to a much greater extent. Exactly how this is achieved remains to be further studied.

4.5. Hypothesis of a Virally Encoded Mutagenic DNA Repair Pathway

While the specific biological functions of most human error-prone DNA polymerases have been demonstrated or hypothesized to involve lesion bypass and/or somatic hypermutation, those of ASFV Pol X are not as well established. Its homology to Pol β, its preference for 5′-phosphorylated gapped DNA,[85,89,90] and the fact that ASFV encodes a B-family DNA polymerase likely to be the replicase[91] all suggest Pol X functions in a viral DNA repair pathway; note that at least one phase of ASFV genome replication/assembly occurs outside the nucleus,[92,93] where host-derived DNA repair factors are expected to be relatively inaccessible. In light of Pol X's error-proneness, we previously hypothesized that the ASFV DNA repair pathway would be mutagenic—helping to confer variability to the viral genome.[89] That Pol X may have evolved specifically to function as a "mutase" during DNA "repair" is supported by the facts that (a) its G:G specificity, i.e., infidelity, is more pronounced on gapped DNA than it is on template/primer DNA (Figure 12B) and (b) it displays low catalytic efficiency—which may be a necessity in that an overly active polymerase/mutase would raise mutagenesis rates to a level incompatible with viability. This hypothetical role of Pol X is consistent with the fact that ASFV displays genetic and antigenic variability which appears to result from, at least in part, an abundance of point mutations.[94]

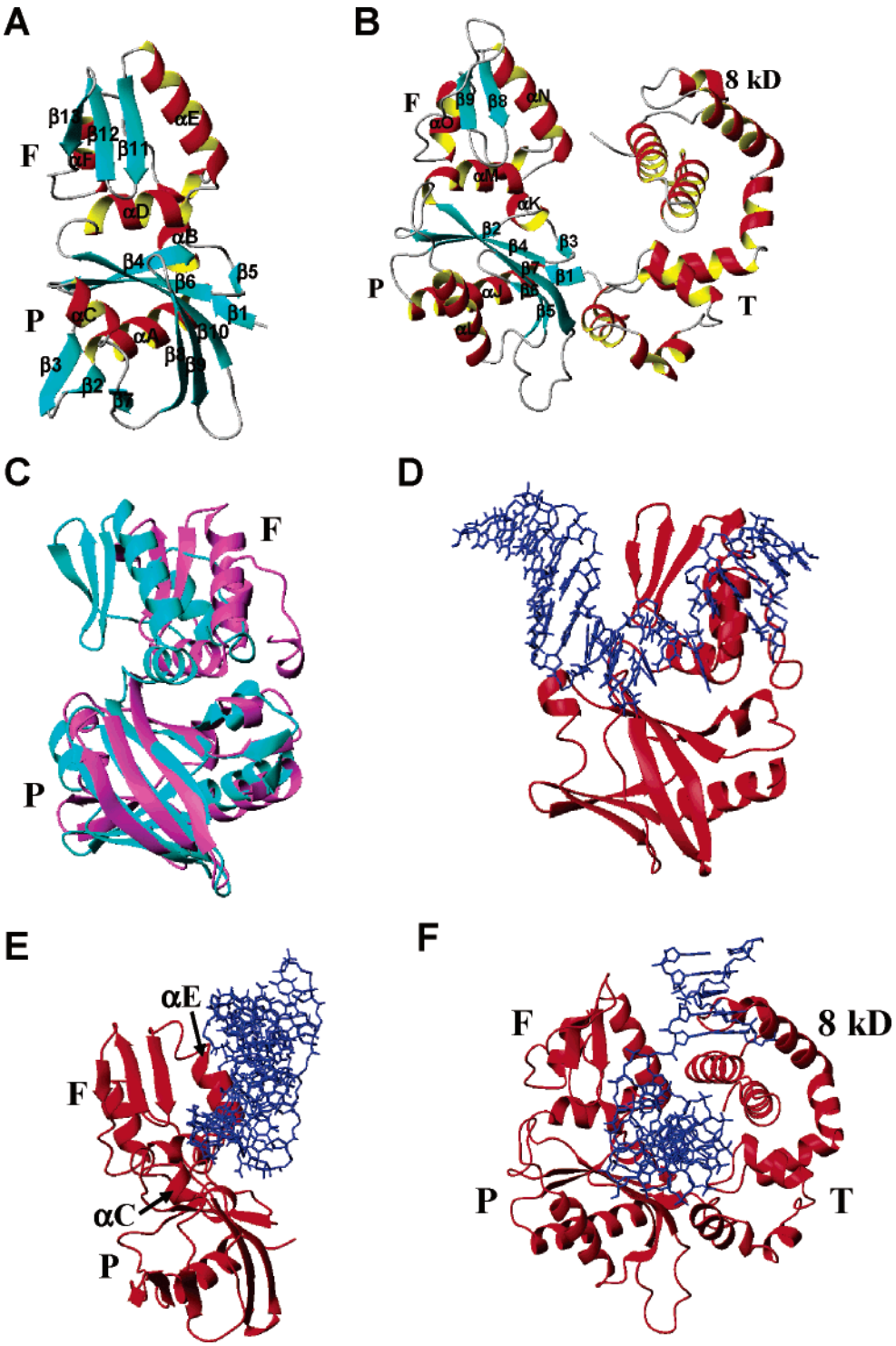

Figure 13. (A) Pol X solution structure (1JAJ). F and P denote the fingers and palm subdomains, according to the notation of Steitz;[121] note that this notation is opposite to that of Pelletier et al.[26] (B) Pol β crystal structure (1BPX), shown in the same orientation (with respect to the three catalytic aspartate residues) as Pol X in part A. 8 kD and T denote the 8 kDa and thumb subdomains, respectively. (C) Solution structures of Pol X in the oxidized (purple) and reduced (blue) forms (1JQR and 1JAJ, respectively);[85,86] to highlight the disulfide-induced structural differences, the orientation of the protein is different here than it is in part A. (D) Solution structure of the Pol X ternary complex with gapped DNA and MgdGTP opposite templating G (the dGTP binding is still being refined, but the enzyme−DNA interaction is well defined).[84] (E) Same as part D, but rotated 90° to illustrate the contacts between DNA and Pol X. (F) Crystal structure of the Pol β ternary complex (1BPY), shown in the same orientation (with respect to the three catalytic aspartate residues) as Pol X in part E.

In order for the low fidelity of Pol X to be biologically relevant, it would need to function within the context of a complete DNA repair pathway in which each of the components tolerated and/or utilized the mismatched intermediates and products generated. Of particular importance is the DNA ligation step, since nick sealing represents a second step (after polymerization) at which mismatches could be discriminated against, tolerated, or even promoted. In section 5, using the ASFV DNA ligase as an example, we present an examination of DNA ligation fidelity. In section 6 the completeness of the ASFV DNA repair system, and its potential mutagenicity, are considered.

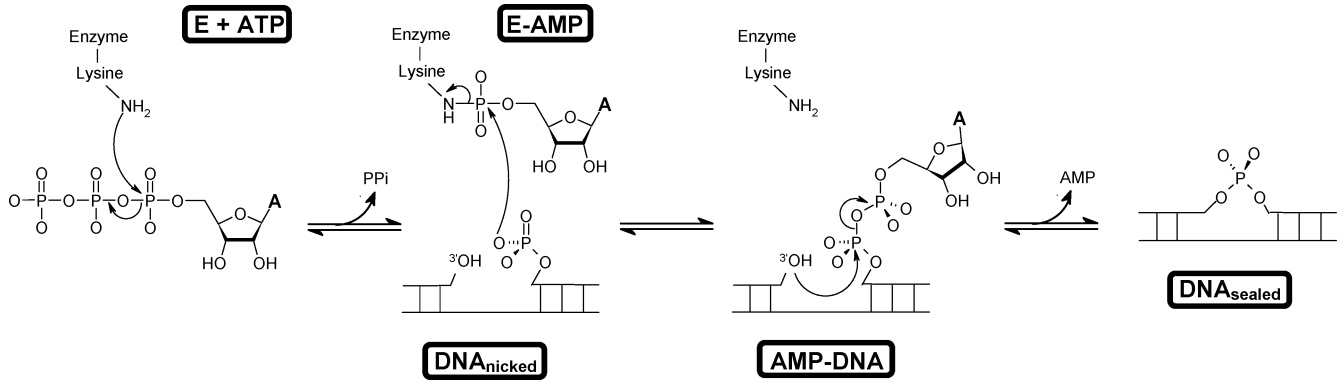

Figure 14. ATP-dependent DNA ligase mechanism. A catalytic lysine attacks the α-phosphate of ATP, generating a lysyl−AMP adduct and releasing pyrophosphate. The conformational change that is apparently induced during this step is not indicated in this scheme. Adenylylated ligase then binds nicked DNA and transfers the AMP group from lysine to the 5′-phosphate of the nick. The 3′-hydroxyl of the nick then attacks the adenylylated 5′-phosphate, forming a phosphodiester bond and eliminating AMP. Finally, cofactor and sealed DNA product are released.

5. Error-Prone DNA Ligation

5.1. Background

Employment of an error-prone polymerase in DNA repair processes—which is hypothesized to fuel diversification of ASFV and may also be the mechanism underlying somatic hypermutation—can give rise to nicks containing 3′ mismatched base pairs. How these mismatched nicks are subsequently processed is the focus of the final two sections of this review (sections 5 and 6). Whereas DNA polymerase fidelity addresses the ability to selectively incorporate the correct nucleotide, the fidelity of DNA ligation pertains to discrimination between nicks containing matched vs mismatched base pairs. After a brief introduction to DNA ligation (section 5.2), we (a) consider the historical interest in DNA ligation fidelity and discuss the potential mechanistic means for effecting ligation fidelity (section 5.3), (b) describe a complete fidelity analysis for ASFV and T4 DNA ligases (section 5.4), and finally (c) use the empirical data to make conclusions about both the magnitude and the determinants of DNA ligation fidelity (section 5.5).

5.2. DNA Ligation

Playing essential roles in replication (Okazaki fragment processing), repair, and recombination, DNA ligases are ubiquitous in all three kingdoms of life, in addition to being encoded within the genomes of a wide variety of viruses.[95] Despite their diversity in size, sequence, and cofactor usage (either ATP or NAD^+), all DNA ligases characterized to date catalyze metal-dependent phosphodiester bond formation between adjacent 3′-hydroxyl and 5′-phosphoryl termini in duplex DNA via a similar mechanism. In the first step of this reaction the ϵ-NH_2 group of a lysine residue attacks the α-phosphate of ATP (or the pyrophosphate linkage of NAD^+), eliminating pyrophosphate (or NMN^+) and forming an enzyme−AMP intermediate.[96] The structural rearrangements associated with this "charging" process[97−99] appear to facilitate binding of nicked DNA.[100,101] The AMP moiety (also referred to as an adenylyl group) is subsequently transferred to the 5′-phosphate of a DNA nick, thereby activating it for nucleophilic attack by the adjacent 3′-hydroxyl.[96] Nick sealing coincides with elimination of AMP and release of the sealed duplex. This reaction mechanism is summarized for an ATP-dependent DNA ligase in Figure 14.

5.3. DNA Ligation Fidelity

Though the biological relevance of mismatch ligation has until recently been questionable,[102] the efficiency of ligating mismatched nicks has been studied semiquantitatively for a large number of DNA ligases.[103−106] These studies of mismatch ligation have been rooted in two major interests: (a) In the technique of ligase detection reaction/ligase chain reaction,[107,108] single-nucleotide polymorphisms are detected based on the ability/inability of a DNA ligase to seal mismatched nicks located at the site of a suspected point mutation. The sensitivity of this technique is determined by the extent to which the DNA ligase discriminates between matches and mismatches either 3′ (upstream), 5′ (downstream), or both 3′ *and* 5′ to the nick. (b) Analysis of mismatch tolerance can be useful for differentiating between the different human enzymes.[104]

Participation of an error-prone DNA polymerase in DNA repair would give rise to nicks containing 3′-OH mismatched base pairs (as opposed to 5′-Pi mismatches) (Figure 15A); accordingly, we focus our discussion on 3′ mismatch ligation exclusively. For a DNA ligase, discrimination against 3′ mismatched nicks might conceptually occur at three different stages of the ligation reaction. That nick sensing/binding would occur without any interaction between the protein and the 3′ base pair seems highly unlikely, so differentiation between match and mismatch might first take place at the level of DNA binding. Second, a ligase, once bound to a nick, might adenylylate the 5′-phosphate with different efficiencies depending on whether the 3′ base pair is matched or mismatched. The reason for this is not immediately obvious, since the positioning of the 5′ phosphate should be relatively immune to the identity of the 3′ base pair. However, the 3′-OH of the nick appears to be a critical component of the active site architecture during adenylylation of the 5′-phosphate—evidenced by the fact that 3′-dideoxy- and 3′-amino-terminated nicks have been found to be *adenylylated* with low efficiency.[102] Third, once nick adenylylation has occurred, a ligase might discriminate between 3′ matched and mismatched base pairs during the final, nick sealing step. The position of the 3′-OH, relative to the adenylylated 5′-phosphate, is expected to vary as a function of 3′ base pair identity; accordingly, the efficiency of the final, nick sealing step is expected to vary with 3′ base pair identity, unless the enzyme is capable of repositioning these reactive moieties. As described in the following sections, it

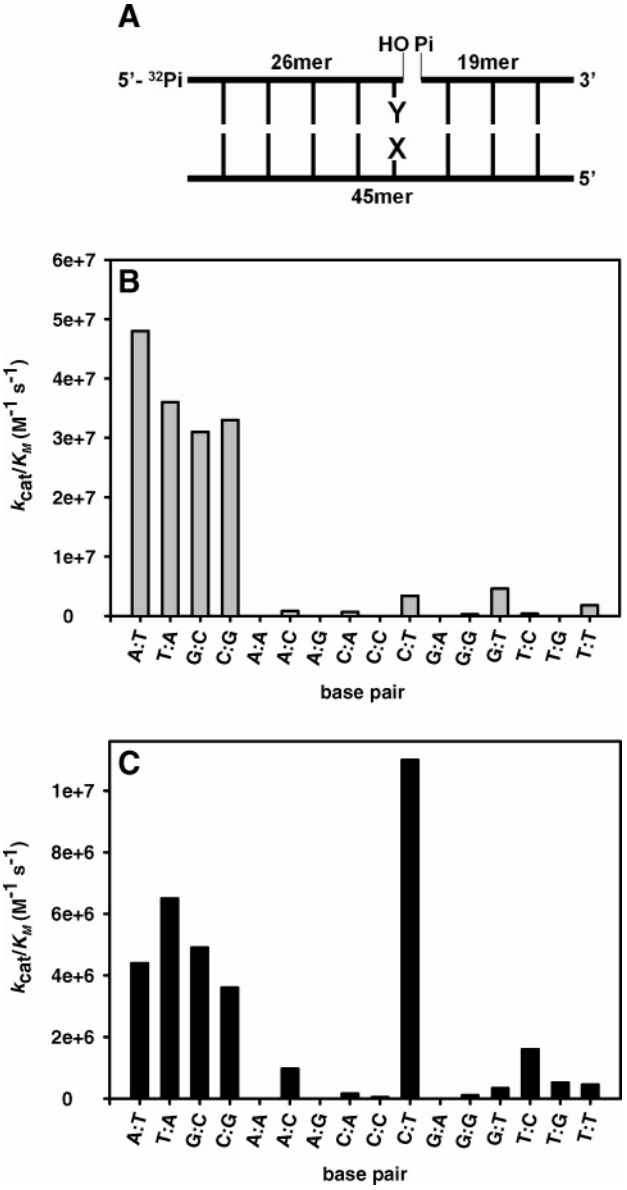

Figure 15. (A) Nicked substrate used in DNA ligation fidelity assays. The 3′ base pair is described by the notation X:Y, where X is the templating nucleotide and Y is the nucleotide that would have been inserted in the preceding gap-filling step. Catalytic efficiencies (k_{cat}/K_M) are plotted as a function of 3′ base pair for T4 DNA ligase (B) and ASFV DNA ligase (C). Note the difference in scale for the *y*-axes. Parts A−C are reproduced with permission from ref 102. Copyright 2005 American Chemical Society.

appears that DNA ligases discriminate against mismatches at all three stages of the nick sealing reaction.

5.4. ASFV DNA Ligase Is Error-Prone

In contrast to DNA polymerases, kinetic analyses of DNA ligase fidelity *using catalytic parameters* are sparse. Most studies have compared the extent of ligation—for match vs mismatch—after a given length of incubation. While this methodology is sufficient for some purposes, it often dramatically overestimates the efficiency of mismatch ligation: at early, unmonitored time points, the ratio [ligated match]/[ligated mismatch] may be very high, but given a long enough incubation period, it may approach unity. To evaluate DNA ligation fidelity as accurately as possible, we previously determined the steady-state catalytic parameters, k_{cat} and K_M, for nick ligation by both bacteriophage T4 and ASFV DNA ligases. For both of these enzymes, the catalytic efficiencies of ligating oligonucleotide substrates containing all 16 possible base pairs at the 3′-OH side of a nick[102] are plotted in parts B and C of Figure 15.

The fidelity of DNA ligation is defined here as $(k_{cat}/K_M)_{correct}/(k_{cat}/K_M)_{incorrect}$; this direct ratio is more appropriate to an analysis of DNA ligation fidelity than is the inverse of the error frequency used above for polymerases since, once bound to its DNA substrate, a ligase does not further discriminate among a pool of second substrates. When compared with T4 DNA ligase, ASFV DNA ligase displays lower fidelity for sealing 11 of the 12 possible mismatched nicks.[102] Especially salient, the ASFV enzyme ligates the C:T mismatch 3-fold more efficiently than the corresponding Watson−Crick base pair, C:G (Figure 15C); this is the only reported example of a DNA ligase that preferentially seals a mismatched nick. The significance of the difference in the mismatch specificities of Pol X and ASFV DNA ligase was speculated on previously[102] and will not be considered here.

5.5. Magnitude and Determinants of DNA Ligase Fidelity

Accepting ASFV DNA ligase as atypical and considering T4 DNA ligase alone, it appears that the magnitude of DNA ligation fidelity is lower than that of DNA polymerization. Using the same definition of fidelity as that used above for polymerases (to facilitate comparison), T4 ligase seals mismatches with an average fidelity—when the anomalous A:G mismatch is excluded—of less than 10^3. It will be interesting to see whether the fidelity of other DNA ligases is of similar, or higher, magnitude.

Assay buffer ionic strength is an important determinant of ligation fidelity for human DNA ligases I and III.[103] This is also true for ASFV DNA ligase; the fidelity of C:T mismatch ligation is higher at 150 mM KCl than it is at 100 mM KCl. However, even at 150 mM KCl, C:T is still sealed more efficiently than C:G.[102] The literature is replete with qualitative examples of 3′ mismatch tolerance by a DNA ligase; however, these studies have been conducted at low, nonphysiological ionic strength,[101,104,105,109] a condition expected to enhance mismatch ligation efficiency. Despite this, none of the DNA ligases studied actually seal a mismatch *preferentially*—which highlights the uniqueness of the ASFV enzyme.

Noteworthy trends in Figure 15 are as follows. Base pair size/geometry is a critical determinant of ligation efficiency. Both ASFV and T4 DNA ligases seal the bulky 3′ purine:purine mismatches (A:A, G:G, G:A, and A:G) very inefficiently, which is consistent with what has been published for a diverse set of DNA ligases.[104,105,108,109] In contrast, the smaller purine:pyrimidine, pyrimidine:purine, and pyrimidine:pyrimidine mismatches are generally better tolerated. Though the preferred 3′ mismatch varies from one DNA ligase to the next, G:T, T:G, C:T, and T:C have consistently proven to be well tolerated,[104,105,109] and this is also the case for the ASFV and T4 enzymes. Importantly, the efficiency of sealing the two permutations of a given base pair, such as the mismatched C:T vs T:C, can vary considerably—suggesting that simple base pair shape/geometry is not the sole determinant of ligation efficiency. Similar results have been obtained for both the Tth[108] and the *Chlorella* virus[101] DNA ligases.

The kinetic data for ASFV and T4 DNA ligases indicate that discrimination against mismatches occurs both at the

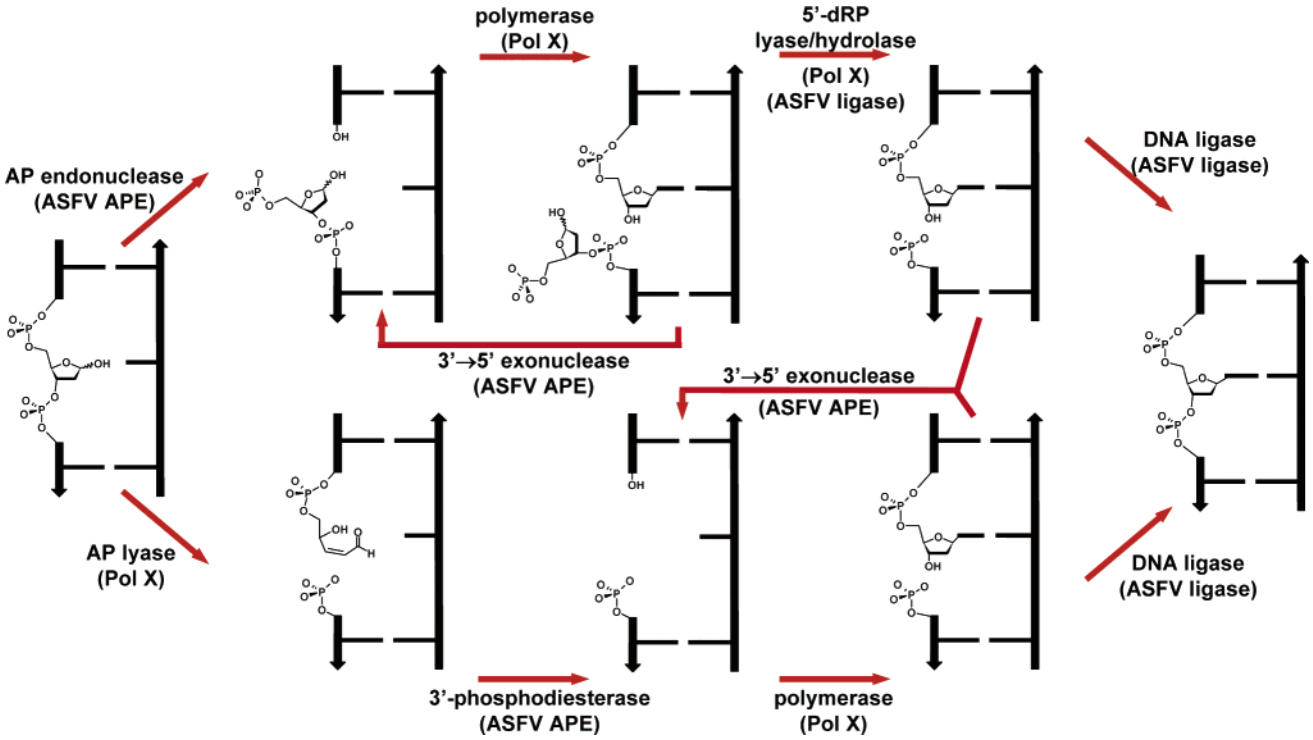

Figure 16. The two routes of the ASFV-encoded AP site repair system. See text for details. Adapted with permission from ref 116.

level of nick binding and during the chemical steps (one or both of the adenylyl transfers involving the DNA nick; it is not possible to differentiate between these since assays were conducted predominantly with the ^{32}P label on the upstream oligonucleotide—precluding detection of the adenylylated DNA intermediate).[102] This is most evident among the four purine:purine mismatches and C:C—all five of which display extremely low k_{cat}'s and high K_M's.[102]

T4 DNA ligase shows an inversion of stereochemistry at the 5′-phosphate during the third step (nick sealing) of DNA ligation.[110] This is consistent with an associative in-line attack of the 5′-phosphate by the 3′-hydroxyl; it is assumed that all ligases operate by a similar mechanism. When the 3′ base pair is a mismatch, the relative positions of the 5′-phosphate and the 3′-hydroxyl are expected to fluctuate. Despite this, the ASFV DNA ligase displays an enhanced k_{cat} with the C:T mismatch (relative to C:G). Accordingly, it would appear that ASFV DNA ligase repositions these reactive groups on the nicked substrate in order to facilitate chemistry. The mechanism by which this is accomplished is unknown at present.

For both *Vaccinia* virus DNA ligase[109] and Tth DNA ligase,[111] mismatch discrimination at the level of DNA binding has been demonstrated. For the latter, use of nucleotide analogues indicated that, analogous to the cases of some DNA polymerases, the relative positioning of minor groove hydrogen-bond acceptors (the N3 nitrogen of the purines and the C2 carbonyl of the pyrimidines) is a critical factor in deciphering between match and mismatch at the 3′ base pair of a nick.[111] It is not yet clear whether this is a universal determinant of DNA ligase fidelity.

Only one structure of a complexed DNA ligase has been solved to date. In this crystal structure of human DNA ligase I bound to an adenylylated nick,[112] the protein shows minimal interaction with the 3′ base pair. This suggests that the protein does not "actively" discriminate between match/mismatch during the third, nick sealing step and that the efficiency of this step ought to depend largely on the relative positions of the 3′-OH and 5′-Pi induced by the local DNA structure. When assayed against the 3′ T:C and T:G mismatches, which ligase I seals with moderate efficiency, the adenylylated DNA intermediate is not detected.[104] Consistent with the conclusion drawn from the structure of the complex, this kinetic result suggests that, at least for these two mismatches, once adenylylation of the nick occurs, the subsequent nick closure step is rapid (i.e. discrimination does not occur during step 3). Since ligase I is a high-fidelity enzyme,[103] it must sense match vs mismatch at earlier steps of the reaction (i.e. DNA binding and/or nick adenylylation).

Since the above-mentioned T:C and T:G assays did not accumulate the adenylylated DNA intermediate,[104] and since ligase I does not interact extensively with the 3′ base pair during the nick sealing step, it would appear that the global distortion the protein imposes on the duplex[112] results in the 3′-OH and the adenylylated 5′-Pi being in positions appropriate for chemistry even when the 3′ base pair is a mismatch. Are there 3′ base pairs, such as the bulkier purine:purine mismatches, for which this is not the case?

In contrast to human ligase I, human ligase III does appear to attain fidelity, at least in part, by discerning match from mismatch during the final, nick sealing step. This protein ligates the T:C and T:G mismatches with reduced efficiency relative to T:A, with concomitant accumulation of the adenylylated DNA intermediate *for the mismatches only*;[104] discrimination against mismatches during the nick sealing step has similarly been observed with the *Vaccinia* virus DNA ligase.[109]

The above discussion provides token examples of ligation fidelity being achieved, at least partially, during three different stages of the nick sealing reaction. On the basis of the limited data currently available, the details of ligation fidelity enforcement appear to vary from one enzyme to the next and are expected to differ as a function of the identity of the 3′ base pair.[111]

6. Complete Abasic Site Repair Pathway in ASFV

6.1. Abasic Site Repair

The fact that ASFV encodes both an error-prone DNA polymerase and an error-tolerant DNA ligase led us to further pursue the potential existence of a complete mutagenic DNA "repair" pathway. Figure 16 outlines the two canonical routes for processing an apurinic/apyrimidinic (AP) site. In the AP endonuclease (APE)-initiated route, an APE incises the sugar phosphate backbone 5′ to an AP site—generating a polymerase-usable single-nucleotide gap containing a 3′-hydroxyl and 5′-deoxyribose phosphate (5′-dRP). In the mammalian system, subsequent gap filling and 5′-dRP removal are both catalyzed by Pol β,[113,114] with either DNA ligase I or III completing repair by sealing the nick.[115] In the alternative AP lyase-initiated route of repair (which Pol X is capable of initiating[83]), the sugar−phosphate backbone is incised 3′ to the AP site—generating a single-nucleotide gap flanked by 5′-phosphate and the polymerase-blocking 3′-4-hydroxy-2-pentenal-5-phosphate. 3-Phosphodiesterase activity, provided at least in part by an APE, generates a polymerase-usable 3′-OH—allowing for gap filling and ligation as described above.

In the following sections we describe the identification and partial characterization of ASFV-encoded activities capable of effecting AP site repair by both the APE and the AP lyase routes, and we provide an assessment of this pathway's mutagenicity.

6.2. AP Endonuclease, 3′-Phosphodiesterase, and 5′-dRP Lyase Activities

Kinetic analyses indicated that the product of ASFV gene *E296R*—which shows sequence homology to *E. coli* endonuclease IV—is a canonical APE which, similar to other APEs, also possesses 3′-phosphodiesterase activity.[116] Though these findings established the existence of a complete ASFV-encoded AP site repair pathway (the AP lyase-initiated route shown in Figure 16), they also presented a conundrum. It was not clear how 5′-dRP, generated upon ASFV APE incision of an AP site, would be removed. The lyase domain of Pol β, which catalyzes 5′-dRP removal in mammals, is entirely absent in its viral homologue Pol X. Though Pol X has been shown to possess lyase activity toward AP sites, a 5′-dRP-removing activity was not identified in a 2003 study.[83] Since 5′-dRP is labile, it might be argued that a catalyst need not participate in this step of AP site processing. However, the half-life for this reaction under physiological conditions is on the order of 30 h,[117] presenting an apparent bottleneck in the ASFV APE-initiated route of AP site repair. 5′-dRP is expected to inhibit DNA ligation by preventing the 5′-phosphate of the nick from being adenylylated. It seemed unlikely that such a metabolic hindrance would be tolerated when the virus retains all other AP site repair activities; accordingly, each of the ASFV DNA repair proteins was assayed for the ability to catalyze 5′-dRP removal. It was found that highly purified forms of both ASFV DNA ligase and Pol X enhance the rate of 5′-dRP loss and do this with similar efficiencies before or after gap filling (i.e. on nicked or gapped substrates).[118] In the presence of sodium borohydride, both proteins form irreversible covalent adducts with 5′-dRP-containing substrates, suggesting that they catalyze this reaction via a lyase (as opposed to a hydrolase) mechanism.[118]

Collectively, the above results demonstrate the ability to carry out AP site repair without the need for host-derived repair factors. An ASFV-encoded enzymatic activity for generating abasic sites has, however, not been identified to date. Accordingly, the AP site processing activities encoded by ASFV may have been retained in order to process lesions generated via spontaneous or chemically induced,[119] rather than enzyme-mediated, base loss; however, the participation of host glycosylases remains a possibility.

6.3. Mismatched Nick Editing Activity

The predominant human AP endonuclease, Ape1, possesses a 3′ → 5′ exonuclease activity that acts preferentially on mismatched nicks.[120] This editing function appears to have evolved for the purpose of enhancing BER fidelity.[120] ASFV APE also possesses 3′ → 5′ exonuclease activity, though the efficiency varies considerably among different mismatches.[116] If the enzymes of the ASFV AP site repair system have coevolved to be collectively mutagenic, then ASFV DNA ligase would be expected to efficiently compete with the exonuclease activity of ASFV APE for mismatched nicks. When incubated simultaneously with equimolar concentrations of ASFV APE and DNA ligase in the presence of magnesium, the C:T mismatch—the preferred substrate for ASFV DNA ligase—is ligated much more efficiently than it is edited. Under identical conditions, the A:G mismatch—the least efficient substrate for ASFV DNA ligase—is edited slightly more efficiently than it is ligated, though a significant extent of ligation is still observed.[118] Human DNA ligases I and III seal mismatched nicks inefficiently[103] and may thereby allow Ape1, or other mismatched nick editors, ample opportunity for proofreading. On the basis of the above preliminary results, the ratio of mismatch ligation to mismatch editing is likely to be higher in the ASFV repair system than in the human repair system.

Besides relative catalytic efficiencies, the fidelity of AP site repair in ASFV will also clearly depend on the relative concentrations of each protein at sites of viral DNA repair. Since no information is available regarding the intracellular concentration of ASFV enzymes, and since ASFV APE is required for virus viability when infecting VERO cells,[83] the influence of ASFV APE on the fidelity of viral DNA repair, and on virus variability in general, remains uncertain.

6.4. Mutagenic DNA Repair for Effecting Genetic Diversification

Though infidelity during replication cannot be discounted (the ASFV replicative polymerase is unstudied in this regard), we have hypothesized that point mutations introduced during abasic site repair may promote the genetic diversification of ASFV.[86,89,102,116] Retention of the ASFV APE, Pol X, and DNA ligase genes in the ASFV genome suggests the usefulness/necessity of these proteins in viral DNA repair (the replacement of a chemically damaged nucleotide with an undamaged nucleotide). However, the fact that both the Pol X and ASFV DNA ligase proteins display extremely low fidelity is not likely to be coincidental and supports their potential usefulness in viral mutagenesis (by replacing a chemically damaged nucleotide with an undamaged, though incorrect, nucleotide).

7. Conclusion and Future Prospects

While this review describes a wealth of mechanistic studies and comparisons of the mechanisms between high-fidelity

and error-prone DNA polymerases and DNA ligases involved in DNA repair, it also makes a point that there is a long way to go before these issues are fully understood. The advancement in the understanding of biological functions of these enzymes has presented a new challenge and new opportunity for chemists and biochemists to uncover the chemical, structural, and kinetic bases of these biological functions. Until a few years ago most research in DNA polymerases and ligases focused on Watson−Crick base pairs of high-fidelity enzymes. In the future we need to shift our effort to understanding how these enzymes differentiate correct from incorrect dNTPs and how the low-fidelity polymerases and ligases differ from the high-fidelity enzymes.

8. List of Abbreviations

2AP	2′-deoxy-2-aminopurine
5′-dRP	5′-deoxyribose phosphate
AP	apurinic/apyrimidinic site
APE	AP endonuclease
ASFV	African swine fever virus
BER	base excision repair
dNTPαS	2′-deoxycytidine-5′-*O*-(1-thiotriphosphate)
dTMPPCP	2′-deoxythymidine-5′-β,γ-methylene-triphosphate
KF	Klenow fragment of *E. coli* DNA polymerase I
MdNTP	generic metal ion 2′-deoxynucleoside-5′-triphosphate complex
MgdNTP	magnesium ion 2′-deoxynucleoside-5′-triphosphate complex
NMR	nuclear magnetic resonance
Pol β	DNA polymerase β
Pol X	DNA polymerase X
SAXS	small-angle X-ray scattering
SHM	somatic hypermutation

9. Acknowledgments

The work from the authors' labs was supported by NIH Research Grant GM43268 and in part by the Genomics Research Center and the NMR Core Facility of Academia Sinica, Taiwan. SAXS experiments were carried out at beamline 4-2 of the Stanford Synchrotron Radiation Laboratory and beamline 18-ID of the Advanced Photon Source, supported by the NIH and the DOE. We thank other coworkers and collaborators, whose work has contributed to this article as cited in the references. The first two authors contributed equally to this review and are thus considered co-first authors.

10. References

(1) Beard, W. A.; Wilson, S. H. *Chem. Rev.* **2006**, *106*, xxxx.
(2) Kunkel, T. A. *J. Biol. Chem.* **2004**, *279*, 16895.
(3) Joyce, C. M.; Benkovic, S. J. *Biochemistry* **2004**, *43*, 14317.
(4) Beard, W. A.; Wilson, S. H. *Structure* **2003**, *11*, 489.
(5) Goodman, M. F. *Annu. Rev. Biochem.* **2002**, *71*, 17.
(6) Rattray, A. J.; Strathern, J. N. *Annu. Rev. Genet.* **2003**, *37*, 31.
(7) Tippin, B.; Pham, P.; Goodman, M. F. *Trends Microbiol.* **2004**, *12*, 288.
(8) Johnson, K. A. *Annu. Rev. Biochem.* **1993**, *62*, 685.
(9) Roberts, J. D.; Kunkel, T. A. *Environ. Mutagen.* **1986**, *8*, 769.
(10) Patel, S. S.; Wong, I.; Johnson, K. A. *Biochemistry* **1991**, *30*, 511.
(11) Dahlberg, M. E.; Benkovic, S. J. *Biochemistry* **1991**, *30*, 4835.
(12) Kuchta, R. D.; Benkovic, P.; Benkovic, S. J. *Biochemistry* **1988**, *27*, 6716.
(13) Doublie, S.; Sawaya, M. R.; Ellenberger, T. *Structure* **1999**, *7*, R31.
(14) Sawaya, M. R.; Prasad, R.; Wilson, S. H.; Kraut, J.; Pelletier, H. *Biochemistry* **1997**, *36*, 11205.
(15) Werneburg, B. G.; Ahn, J.; Zhong, X.; Hondal, R. J.; Kraynov, V. S.; Tsai, M.-D. *Biochemistry* **1996**, *35*, 7041.
(16) Zhong, X.; Patel, S. S.; Tsai, M.-D. *J. Am. Chem. Soc.* **1998**, *120*, 235.
(17) Zhong, X.; Patel, S. S.; Werneburg, B. G.; Tsai, M.-D. *Biochemistry* **1997**, *36*, 11891.
(18) Arndt, J. W.; Gong, W.; Zhong, X.; Showalter, A. K.; Liu, J.; Dunlap, C. A.; Lin, Z.; Paxson, C.; Tsai, M.-D.; Chan, M. K. *Biochemistry* **2001**, *40*, 5368.
(19) Showalter, A. K.; Tsai, M.-D. *Biochemistry* **2002**, *41*, 10571.
(20) Yang, L.; Beard, W. A.; Wilson, S. H.; Broyde, S.; Schlick, T. *J. Mol. Biol.* **2002**, *317*, 651.
(21) Dunlap, C. A.; Tsai, M.-D. *Biochemistry* **2002**, *41*, 11226.
(22) Gavish, B.; Werber, M. M. *Biochemistry* **1979**, *18*, 1269.
(23) Bakhtina, M.; Lee, S.; Wang, Y.; Dunlap, C. A.; Lamarche, B. J.; Tsai, M.-D. *Biochemistry* **2005**, *44*, 5177.
(24) Bakhtina, M.; Tsai, M.-D. in preparation.
(25) Yang, L.; Arora, K.; Beard, W. A.; Wilson, S. H.; Schlick, T. *J. Am. Chem. Soc.* **2004**, *126*, 8441.
(26) Pelletier, H.; Sawaya, M. R.; Kumar, A.; Wilson, S. H.; Kraut, J. *Science* **1994**, *264*, 1891.
(27) Sawaya, M. R.; Pelletier, H.; Kumar, A.; Wilson, S. H.; Kraut, J. *Science* **1994**, *264*, 1930.
(28) Bose-Basu, B.; DeRose, E. F.; Kirby, T. W.; Mueller, G. A.; Beard, W. A.; Wilson, S. H.; London, R. E. *Biochemistry* **2004**, *43*, 8911.
(29) (a) Tang, K.-H.; Tsai, M.-D. manuscript in preparation. (b) Semenyuk, A. V.; Svergun, D. I. *J. Appl. Crystallogr.* **1991**, *24*, 537.
(30) Krahn, J. M.; Beard, W. A.; Wilson, S. H. *Structure* **2004**, *12*, 1823.
(31) Purohit, V.; Grindley, N. D. F.; Joyce, C. M. *Biochemistry* **2003**, *42*, 10200.
(32) Radhakrishnan, R.; Schlick, T. *J. Am. Chem. Soc.* **2005**, *127*, 13245.
(33) Vande Berg, B. J.; Beard, W. A.; Wilson, S. H. *J. Biol. Chem.* **2001**, *276*, 3408.
(34) Kim, S.-J.; Beard William, A.; Harvey, J.; Shock David, D.; Knutson Jay, R.; Wilson Samuel, H. *J. Biol. Chem.* **2003**, *278*, 5072.
(35) Arora, K.; Beard, W. A.; Wilson, S. H.; Schlick, T. *Biochemistry* **2005**, *44*, 13328.
(36) Wong, I.; Patel, S. S.; Johnson, K. A. *Biochemistry* **1991**, *30*, 526.
(37) Herschlag, D.; Piccirilli, J. A.; Cech, T. R. *Biochemistry* **1991**, *30*, 4844.
(38) Knowles, J. R. *Annu. Rev. Biochem.* **1980**, *49*, 877.
(39) Rothwell, P. J.; Mitaksov, V.; Waksman, G. *Mol. Cell* **2005**, *19*, 345.
(40) Florian, J.; Goodman, M. F.; Warshel, A. *Proc. Natl. Acad. Sci. U.S.A.* **2005**, *102*, 6819.
(41) Ohmori, H.; Friedberg, E. C.; Fuchs, R. P. P.; Goodman, M. F.; Hanaoka, F.; Hinkle, D.; Kunkel, T. A.; Lawrence, C. W.; Livneh, Z.; Nohmi, T.; Prakash, L.; Prakash, S.; Todo, T.; Walker, G. C.; Wang, Z.; Woodgate, R. *Mol. Cell* **2001**, *8*, 7.
(42) Johnson, R. E.; Washington, M. T.; Haracska, L.; Prakash, S.; Prakash, L. *Nature* **2000**, *406*, 1015.
(43) Haracska, L.; Prakash, S.; Prakash, L. *Mol. Cell. Biol.* **2003**, *23*, 1453.
(44) Washington, M. T.; Minko, I. G.; Johnson, R. E.; Haracska, L.; Harris, T. M.; Lloyd, R. S.; Prakash, S.; Prakash, L. *Mol. Cell. Biol.* **2004**, *24*, 6900.
(45) Fiala, K. A.; Abdel-Gawad, W.; Suo, Z. *Biochemistry* **2004**, *43*, 6751.
(46) Matsuda, T.; Bebenek, K.; Masutani, C.; Hanaoka, F.; Kunkel, T. A. *Nature* **2000**, *404*, 1011.
(47) McCulloch, S. D.; Kokoska, R. J.; Masutani, C.; Iwai, S.; Hanaoka, F.; Kunkel, T. A. *Nature* **2004**, *428*, 97.
(48) Ohashi, E.; Bebenek, K.; Matsuda, T.; Feaver, W. J.; Gerlach, V. L.; Friedberg, E. C.; Ohmori, H.; Kunkel, T. A. *J. Biol. Chem.* **2000**, *275*, 39678.
(49) Yang, I.-Y.; Miller, H.; Wang, Z.; Frank, E. G.; Ohmori, H.; Hanaoka, F.; Moriya, M. *J. Biol. Chem.* **2003**, *278*, 13989.
(50) Zhang, Y.; Yuan, F.; Wu, X.; Wang, Z. *Mol. Cell. Biol.* **2000**, *20*, 7099.
(51) Zhang, Y.; Yuan, F.; Xin, H.; Wu, X.; Rajpal, D. K.; Yang, D.; Wang, Z. *Nucleic Acids Res.* **2000**, *28*, 4147.
(52) (a) Zhang, Y.; Yuan, F.; Wu, X.; Wang, M.; Rechkoblit, O.; Taylor, J.-S.; Geacintov, N. E.; Wang, Z. *Nucleic Acids Res.* **2000**, *28*, 4138. (b) Ogi, T.; Shinkai, Y.; Tanaka, K.; Ohmori, H. *Proc. Natl. Acad. Sci. U.S.A.* **2002**, *99*, 15548.
(53) Carlson, K. D.; Washington, M. T. *Mol. Cell. Biol.* **2005**, *25*, 2169.
(54) Bebenek, K.; Tissier, A.; Frank, E. G.; McDonald, J. P.; Prasad, R.; Wilson, S. H.; Woodgate, R.; Kunkel, T. A. *Science* **2001**, *291*, 2156.
(55) Roettger, M. P.; Fiala, K. A.; Sompalli, S.; Dong, Y.; Suo, Z. *Biochemistry* **2004**, *43*, 13827.
(56) Vaisman, A.; Tissier, A.; Frank, E. G.; Goodman, M. F.; Woodgate, R. *J. Biol. Chem.* **2001**, *276*, 30615.
(57) Washington, M. T.; Johnson, R. E.; Prakash, L.; Prakash, S. *Mol. Cell. Biol.* **2003**, *23*, 8316.
(58) Washington, M. T.; Johnson, R. E.; Prakash, L.; Prakash, S. *Mol. Cell. Biol.* **2004**, *24*, 936.
(59) Washington, M. T.; Prakash, L.; Prakash, S. *Cell* **2001**, *107*, 917.

(60) Sun, L.; Zhang, K.; Zhou, L.; Hohler, P.; Kool, E. T.; Yuan, F.; Wang, Z.; Taylor, J. S. *Biochemistry* **2003**, *42*, 9431.
(61) Washington, M. T.; Prakash, L.; Prakash, S. *Proc. Natl. Acad. Sci. U.S.A.* **2003**, *100*, 12093.
(62) Washington, M. T.; Wolfle, W. T.; Spratt, T. E.; Prakash, L.; Prakash, S. *Proc. Natl. Acad. Sci. U.S.A.* **2003**, *100*, 5113.
(63) Hwang, H.; Taylor, J.-S. *Biochemistry* **2005**, *44*, 4850.
(64) Glick, E.; Chau, J. S.; Vigna, K. L.; McCulloch, S. D.; Adman, E. T.; Kunkel, T. A.; Loeb, L. A. *J. Biol. Chem.* **2003**, *278*, 19341.
(65) Fiala, K. A.; Suo, Z. *Biochemistry* **2004**, *43*, 2116.
(66) Fiala, K. A.; Suo, Z. *Biochemistry* **2004**, *43*, 2106.
(67) Tippin, B.; Kobayashi, S.; Bertram, J. G.; Goodman, M. F. *J. Biol. Chem.* **2004**, *279*, 45360.
(68) Beard, W. A.; Shock, D. D.; Vande Berg, B. J.; Wilson, S. H. *J. Biol. Chem.* **2002**, *277*, 47393.
(69) Garcia-Diaz, M.; Bebenek, K.; Krahn, J. M.; Blanco, L.; Kunkel, T. A.; Pedersen, L. C. *Mol. Cell* **2004**, *13*, 561.
(70) Garcia-Diaz, M.; Bebenek, K.; Krahn, J. M.; Kunkel, T. A.; Pedersen, L. C. *Nat. Struct. Mol. Biol.* **2005**, *12*, 97.
(71) Ling, H.; Boudsocq, F.; Plosky, B. S.; Woodgate, R.; Yang, W. *Nature* **2003**, *424*, 1083.
(72) Ling, H.; Boudsocq, F.; Woodgate, R.; Yang, W. *Cell* **2001**, *107*, 91.
(73) Ling, H.; Boudsocq, F.; Woodgate, R.; Yang, W. *Mol. Cell* **2004**, *13*, 751.
(74) Ling, H.; Sayer, J. M.; Plosky, B. S.; Yagi, H.; Boudsocq, F.; Woodgate, R.; Jerina, D. M.; Yang, W. *Proc. Natl. Acad. Sci. U.S.A.* **2004**, *101*, 2265.
(75) Nair, D. T.; Johnson, R. E.; Prakash, S.; Prakash, L.; Aggarwal, A. K. *Nature* **2004**, *430*, 377.
(76) Trincao, J.; Johnson, R. E.; Escalante, C. R.; Prakash, S.; Prakash, L.; Aggarwal, A. K. *Mol. Cell* **2001**, *8*, 417.
(77) Trincao, J.; Johnson, R. E.; Wolfle, W. T.; Escalante, C. R.; Prakash, S.; Prakash, L.; Aggarwal, A. K. *Nat. Struct. Mol. Biol.* **2004**, *11*, 457.
(78) Uljon, S. N.; Johnson, R. E.; Edwards, T. A.; Prakash, S.; Prakash, L.; Aggarwal, A. K. *Structure* **2004**, *12*, 1395.
(79) Zhou, B.-L.; Pata, J. D.; Steitz, T. A. *Mol. Cell* **2001**, *8*, 427.
(80) Boudsocq, F.; Kokoska, R. J.; Plosky, B. S.; Vaisman, A.; Ling, H.; Kunkel, T. A.; Yang, W.; Woodgate, R. *J. Biol. Chem.* **2004**, *279*, 32932.
(81) Washington, M. T.; Minko, I. G.; Johnson, R. E.; Wolfle, W. T.; Harris, T. M.; Lloyd, R. S.; Prakash, S.; Prakash, L. *Mol. Cell. Biol.* **2004**, *24*, 5687.
(82) Yanez, R. J.; Rodriguez, J. M.; Nogal, M. L.; Yuste, L.; Enriquez, C.; Rodriguez, J. F.; Vinuela, E. *Virology* **1995**, *208*, 249.
(83) Garcia-Escudero, R.; Garcia-Diaz, M.; Salas, M. L.; Blanco, L.; Salas, J. *J. Mol. Biol.* **2003**, *326*, 1403.
(84) Su, M.-I.; Kumar, S.; Showalter, A. K.; Byeon, I.-J. L.; Wu, W.-J.; Tsai, M.-D. Unpublished results.
(85) Maciejewski, M. W.; Shin, R.; Pan, B.; Marintchev, A.; Denninger, A.; Mullen, M. A.; Chen, K.; Gryk, M. R.; Mullen, G. P. *Nat. Struct. Biol.* **2001**, *8*, 936.
(86) Showalter, A. K.; Byeon, I.-J. L.; Su, M.-I.; Tsai, M.-D. *Nat. Struct. Biol.* **2001**, *8*, 942.
(87) Casas-Finet, J. R.; Kumar, A.; Karpel, R. L.; Wilson, S. H. *Biochemistry* **1992**, *31*, 10272.
(88) Doublie, S.; Tabor, S.; Long, A. M.; Richardson, C. C.; Ellenberger, T. *Nature* **1998**, *391*, 251.
(89) Showalter, A. K.; Tsai, M.-D. *J. Am. Chem. Soc.* **2001**, *123*, 1776.
(90) Oliveros, M.; Yanez, R. J.; Salas, M. L.; Salas, J.; Vinuela, E.; Blanco, L. *J. Biol. Chem.* **1997**, *272*, 30899.
(91) Rodriguez, J. M.; Yanez, R. J.; Rodriguez, J. F.; Vinuela, E.; Salas, M. L. *Gene* **1993**, *136*, 103.
(92) Brookes, S. M.; Dixon, L. K.; Parkhouse, R. M. E. *Virology* **1996**, *224*, 84.
(93) Rojo, G.; Garcia-Beato, R.; Vinuela, E.; Salas, M. L.; Salas, J. *Virology* **1999**, *257*, 524.
(94) Dixon, L. K.; Wilkinson, P. J. *J. Gen. Virol.* **1988**, *69*, 2981.
(95) Cao, W. *Curr. Org. Chem.* **2002**, *6*, 827.
(96) Lehman, I. R. *Science* **1974**, *186*, 790.
(97) Gajiwala, K. S.; Pinko, C. *Structure* **2004**, *12*, 1449.
(98) Georlette, D.; Blaise, V.; Bouillenne, F.; Damien, B.; Thorbjarnardottir, S. H.; Depiereux, E.; Gerday, C.; Uversky, V. N.; Feller, G. *Biophys. J.* **2004**, *86*, 1089.
(99) Georlette, D.; Blaise, V.; Dohmen, C.; Bouillenne, F.; Damien, B.; Depiereux, E.; Gerday, C.; Uversky, V. N.; Feller, G. *J. Biol. Chem.* **2003**, *278*, 49945.
(100) Odell, M.; Sriskanda, V.; Shuman, S.; Nikolov, D. B. *Mol. Cell* **2000**, *6*, 1183.
(101) Sriskanda, V.; Shuman, S. *Nucleic Acids Res.* **1998**, *26*, 3536.
(102) Lamarche, B. J.; Showalter, A. K.; Tsai, M.-D. *Biochemistry* **2005**, *44*, 8408.
(103) Bhagwat, A. S.; Sanderson, R. J.; Lindahl, T. *Nucleic Acids Res.* **1999**, *27*, 4028.
(104) Husain, I.; Tomkinson, A. E.; Burkhart, W. A.; Moyer, M. B.; Ramos, W.; Mackey, Z. B.; Besterman, J. M.; Chen, J. *J. Biol. Chem.* **1995**, *270*, 9683.
(105) Tomkinson, A. E.; Tappe, N. J.; Friedberg, E. C. *Biochemistry* **1992**, *31*, 11762.
(106) Tong, J.; Cao, W.; Barany, F. *Nucleic Acids Res.* **1999**, *27*, 788.
(107) Barany, F. *Proc. Natl. Acad. Sci. U.S.A.* **1991**, *88*, 189.
(108) Luo, J.; Bergstrom, D. E.; Barany, F. *Nucleic Acids Res.* **1996**, *24*, 3071.
(109) Shuman, S. *Biochemistry* **1995**, *34*, 16138.
(110) Mizuuchi, K.; Nobbs, T. J.; Halford, S. E.; Adzuma, K.; Qin, J. *Biochemistry* **1999**, *38*, 4640.
(111) Liu, P.; Burdzy, A.; Sowers, L. C. *Nucleic Acids Res.* **2004**, *32*, 4503.
(112) Pascal, J. M.; O'Brien, P. J.; Tomkinson, A. E.; Ellenberger, T. *Nature* **2004**, *432*, 473.
(113) Prasad, R.; Beard, W. A.; Strauss, P. R.; Wilson, S. H. *J. Biol. Chem.* **1998**, *273*, 15263.
(114) Srivastava, D. K.; Berg, B. J. V.; Prasad, R.; Molina, J. T.; Beard, W. A.; Tomkinson, A. E.; Wilson, S. H. *J. Biol. Chem.* **1998**, *273*, 21203.
(115) Sleeth, K. M.; Robson, R. L.; Dianov, G. L. *Biochemistry* **2004**, *43*, 12924.
(116) Lamarche, B. J.; Tsai, M.-D. *Biochemistry*, **2006**, in press.
(117) Price, A.; Lindahl, T. *Biochemistry* **1991**, *30*, 8631.
(118) Lamarche, B. J.; Tsai, M.-D., in preparation.
(119) Lindahl, T. *Nature* **1993**, *362*, 709.
(120) Chou, K.-M.; Cheng, Y.-C. *Nature* **2002**, *415*, 655.
(121) Steitz, T. A. *J. Biol. Chem.* **1999**, *274*, 17395.

CR040487K